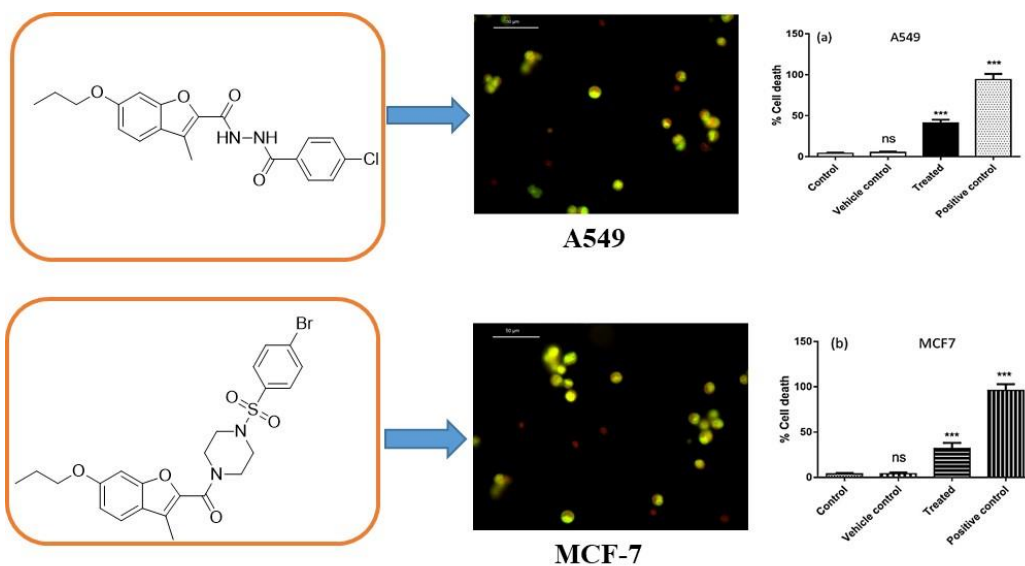


Chapter-2

Design, Synthesis and Anticancer Activity of Amide Derivatives of Substituted 3-Methyl-benzofuran-2-carboxylic acid



2.1 Introduction

Cancer, a complex and heterogeneous group of diseases characterized by uncontrolled cell growth and proliferation, constitutes a significant global health challenge [1]. Among its numerous types, lung cancer and breast cancer stand out as two prominent and extensively studied subtypes. Lung cancer, often associated with tobacco smoke and environmental pollutants, poses a major public health concern due to its aggressive nature and limited treatment options at advanced stages. In contrast, breast cancer, influenced by genetic, hormonal, and lifestyle factors, represents the most diagnosed cancer in women globally. Advances in research and medical interventions have led to improved detection, targeted therapies, and personalized treatment approaches for both lung and breast cancers, underscoring the critical importance of continued investigation and innovation in addressing these pressing health issues.

Benzofuran, is one of the important heterocyclic compound known as natural as well as synthetic compound, holds significant importance in various scientific and industrial domains. Its unique structural arrangement and versatile reactivity makes it a valuable building block for the synthesis of diverse pharmaceuticals, agrochemicals, and materials. Benzofuran derivatives exhibit a wide range of biological activities, including antimicrobial [2], antifungal [3], anti-inflammatory [4], antioxidant [5] and antiviral agent [6]. thereby contributing to advancements in drug discovery and development. During last few decades, benzofuran carboxylic acid derivatives have been reported having potent anticancer activity with low side effects and better solubility for therapeutic applications. Additionally, their interactions with biological targets offer insights into structure-activity relationships and molecular mechanisms. The exploration of benzofuran carboxylic acids as therapeutic agents with multifaceted biological activities holds great promise for addressing various health challenges and advancing the field of medicinal chemistry. Benzofuran derivatives exhibited antitumor activities at different stages of cancer formation through various mechanisms, for example blocking cell cycle, inducing cell apoptosis, modulating estrogen receptor [7]. Literature search reveals that benzofuran carboxamide derivatives have showed very good anticancer activity [8].

There are few reports of synthetic benzofuran derivatives as an anticancer agent against breast cancer cell line(MCF-7) and lung cancer cell line(A549). Sandra *et al.* reported novel heterocyclic derivatives of benzofuran-2-carboxamides containing compound **1** (Figure-2.1), having good anticancer activity with IC_{50} value $7 \mu M$ against MCF-7 cell line and induced

apoptosis [9]. Further modifications were made by various researchers to enhance activity of benzofuran. Qi-dong *et al.* reported compounds **2a** and **2b**s (Figure-2.1) exhibited excellent cytotoxicity against many cancer cell lines, including MCF-7 and A549 with IC_{50} values 2.39 μ M and 3.08 μ M respectively [10]. The research is ongoing on development of new active anticancer compounds by changing the position of the substituent attached to the benzofuran. Recently Mohammad *et al.* reported compound **4** (Figure-2.1) as potential anticancer agent towards A549 cell lines, the target benzofuran-based derivatives efficiently inhibited the growth of A549 cell lines with IC_{50} value 3.69 μ M and also further investigated for their effects on the cell cycle progression and apoptosis in A549 cell line [11].

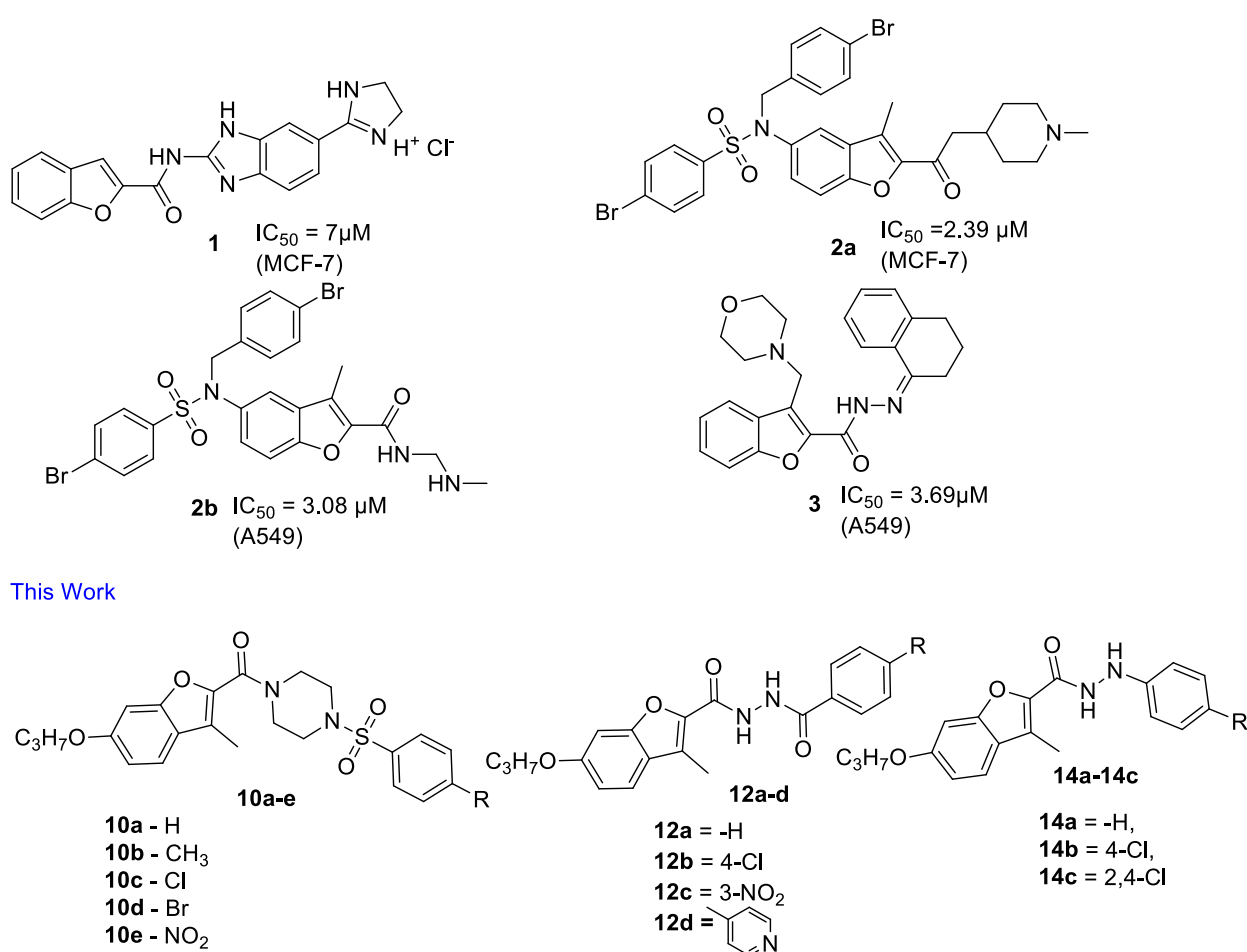


Figure-2.1 Benzofuran derivatives with anticancer activity

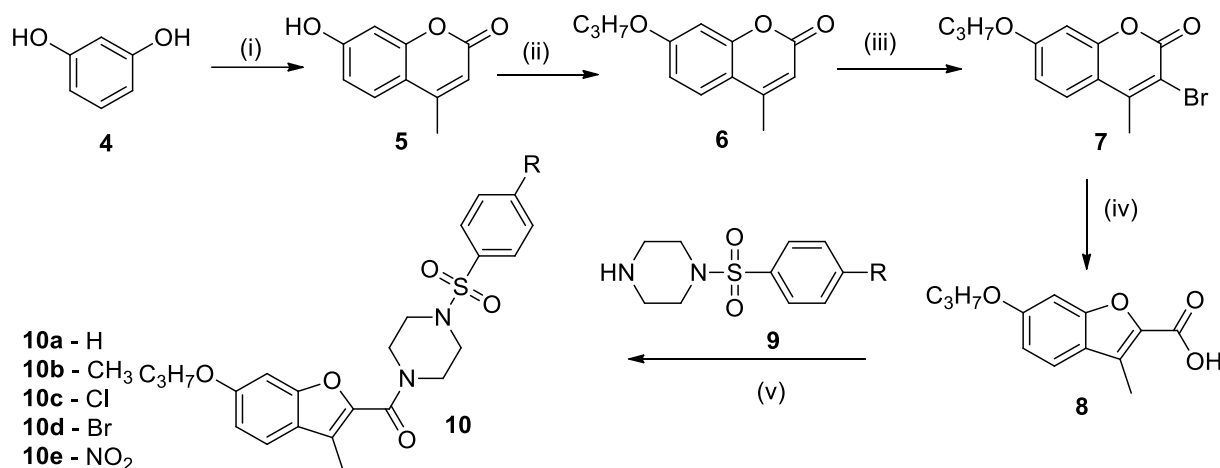
The pharmacological properties and applications of benzofuran derivatives can be tuned by varying type and position of substitution on furan ring. However, there are limited reports on benzofuran carboxamide derivatives with different substituted phenyl hydrazine, phenyl hydrazides and no reports were found on amide derivatives of benzofuran carboxylic acid with different phenyl sulphonyl piperazines. Due to potential applications of benzofuran derivatives

and as a part of our continuous efforts to design and develop novel derivatives for anticancer activity [12-13], we report herein synthesis of various amide derivatives of 3-methyl benzofuran carboxylic acid and studied them for their anticancer activity, cytotoxicity and drug likeness (**Fig-2.1**).

2.2 Results and Discussion

2.2.1 Chemistry

In search of some novel compounds with potent anticancer activity, compounds **10a-e** have been synthesized from 3-methyl-6-propoxybenzofuran-2-carboxylic acid **8**. Compound **8** synthesized in four steps starting with 7-Hydroxy-4-methyl coumarin **5** which was prepared via Pechmann condensation of resorcinol **4** with ethyl acetoacetate in presence of conc. H_2SO_4 . Compound **5** was O-alkylated using propyl bromide in presence of K_2CO_3 and DMF with pinch of KI to give 7-propoxy-4-methylcoumarin **6** (**Scheme-1**).



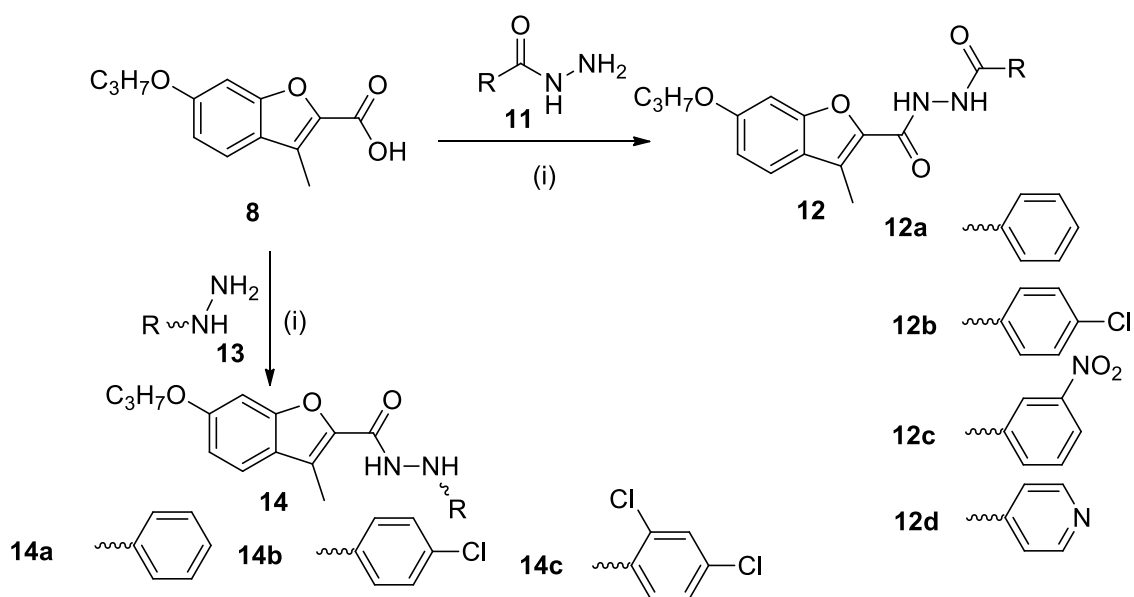
Reagents & conditions: (i) Ethyl acetoacetate, conc. H_2SO_4 ; rt 5-6 hr (ii) C_3H_7Br , K_2CO_3 , KI, DMF, rt, 8-10hr; (iii) Br_2 in glacial acetic acid, rt 8-12hr; (iv) 10% ethanolic KOH, reflux 3hr (v) HOBt, EDC, TEA, DCM 6hr.

Scheme 1: Benzofuran derivatives **10a-e**

Bromination of compound **6** was carried out by using bromine in glacial acetic acid at room temperature to give 3-bromo-4-methyl-7-propoxy coumarin **7**. Compound **7** was refluxed with 10% ethanolic KOH for 3 hours to give 6-propoxy-3-methyl benzofuran-2 carboxylic acid **8** via Perkin rearrangement. Compound **8** on reaction with different arylsulfonamide piperazines derivatives using EDC, HOBt and TEA in dichloromethane gave final compounds **10a-e**. All the synthesized compounds were characterized by different spectral techniques such as 1H -NMR, ^{13}C -NMR, IR, ESI-MS and CHN analysis.

In general, the IR spectra of compounds **10a** to **10e** exhibited two strong bands in the range of $2840-3060\text{ cm}^{-1}$ for $-CH$ stretching of propyl chain, and at $1611-1670\text{ cm}^{-1}$ for amide carbonyl

stretching frequency. In $^1\text{H-NMR}$ spectrum of compound **10b**, the triplet for $-\text{CH}_3$ of propyl chain is observed at δ 1.07, the multiplet for CH_2- of propyl chain is observed at δ 1.84. The singlet for three protons of methyl on furan ring is observed at δ 2.41 (**Fig-2.4.2**) The triplet for two methylenoxy protons is observed at δ 3.9. All aromatic protons observed in the range of δ 6.92-7.67. In $^{13}\text{C-NMR}$ of compound **10b** the $-\text{CH}_3$ carbons observed at δ 9.26 and 22.51, the methylene carbons were observed at δ 10.56 and 70.06 ppm. All the aromatic carbons were observed between δ 96.08-160.89 ppm (**Fig-2.4.3**) along with amide carbonyl carbon observed at δ 160.89. The ESI-Mass spectrum of compound **10b** showed $[\text{M}+\text{H}]^+$ peak at 457.10. (**Fig-2.4.4**) In general, for $^1\text{H-NMR}$ of compounds **10a-e** the triplet, multiplet for $-\text{CH}_3-\text{CH}_2$ are observed in the range of δ 1.07-1.11 and δ 1.77- 1.85 respectively. Singlet for three protons of methyl group attached to aromatic furan ring is observed in the range of δ 2.40-2.41 ppm, methylene protons which are attached to oxygen are observed in the range of δ 3.89-3.99, all aromatic protons observed in the range of δ 6.91- 8.44 ppm. In $^{13}\text{C-NMR}$ spectra of compounds **10a-e**, the methyl carbons were observed at δ 9.25 and δ 22.51 and methylene carbons were observed at δ 10.93, and δ 70.06 ppm, all aromatic carbons were observed in the range of δ 96.00-161.05 ppm along with amide carbonyl carbon.



Scheme 2: Benzofuran derivatives **12a-d** and **14a-c**

Compound **8** (3-methyl-6-propoxy benzofuran 2-carboxylic acid) was reacted with various substituted aryl hydrazides **11** in presence of EDC, HOBT, TEA in DCM to give corresponding (**Scheme-2**) different substituted dihydrazides derivatives of furan carboxylic acid **12a-d**. In

another variation, benzofuran carboxylic acid **8** was reacted with different substituted aryl hydrazines **13** under similar reaction conditions to give compounds **14a-c** (Scheme 2). The structures of all the compounds were confirmed by its IR, $^1\text{H-NMR}$, $^{13}\text{C-NMR}$, ESI-Mass spectra.

In IR spectra of **12a-d**, one band for -NH stretching was observed from $3200\text{-}3450\text{ cm}^{-1}$, while -CH stretching of propyl chain was observed around $2840\text{-}3060\text{ cm}^{-1}$. The amide carbonyl band was observed at $1622\text{-}1675\text{ cm}^{-1}$. In the $^1\text{H-NMR}$ spectrum of **12b** (Fig-2.9.2) the -CH₃ protons of propyl chain are observed as triplet at δ 1.03 and -CH₂ protons as multiplet at δ 1.84 and -OCH₂ protons as triplet at δ 4.06. The methyl protons of furan ring were observed at δ 2.50-2.55. All aromatic protons were observed in range of δ 6.94-10.65 ppm along with two -NH protons were appeared at δ 10.50 and 10.62 ppm respectively, which was confirmed by D₂O exchange study. In $^{13}\text{C-NMR}$ spectrum of compound **12b** (Fig-2.9.3) showed two methyl carbons at δ 9.24 and δ 22.46, -CH₂ carbon at δ 10.93 and -CH₂ attached to oxygen atom at δ 70.04 ppm. All aromatic carbons were observed in the range of δ 96.04-165.25 along with amide carbonyl carbon observed at δ 165.25 ppm respectively. The ESI-Mass of **12b** showed [M⁺] peak at 386.60 (Fig-2.9.4).

In IR spectra of compounds **14a-c**, one band is observed for -NH stretching frequencies at 3058 cm^{-1} and two bands for -CH stretching of propyl chain, at 3010 and 2854 cm^{-1} respectively. The amide carbonyl stretching frequency was observed at $1650\text{-}1673\text{ cm}^{-1}$. In $^1\text{H-NMR}$ spectrum of **14c** (Fig-2.16.2) the CH₃-CH₂-protons of propyl chain were observed as triplet and multiplet at δ 1.11, δ 1.90 respectively and The triplet for two methylene protons observed at δ 4.01 which is attached to oxygen, the -CH₃ protons of furan methyl were observed as singlet at δ 2.58 all aromatic protons observed in the range of δ 6.58-8.32. In $^{13}\text{C-NMR}$ spectrum of compound **14c** (Fig-2.16.3) showed two methyl carbons at δ 9.01 and δ 22.50, two -CH₂ carbons at δ 10.57, and δ 70.09 ppm respectively. All aromatic carbons were observed in the range of δ 96.05-160.30 with amide carbonyl carbons are observed at δ 160.3 The ESI-Mass of **14c** showed [M⁺] peak at 393.00 (Fig-2.16.4).

Figure- 2.3.1 IR of 3-methyl-6-propoxybenzofuran-2-carboxylic acid (8)

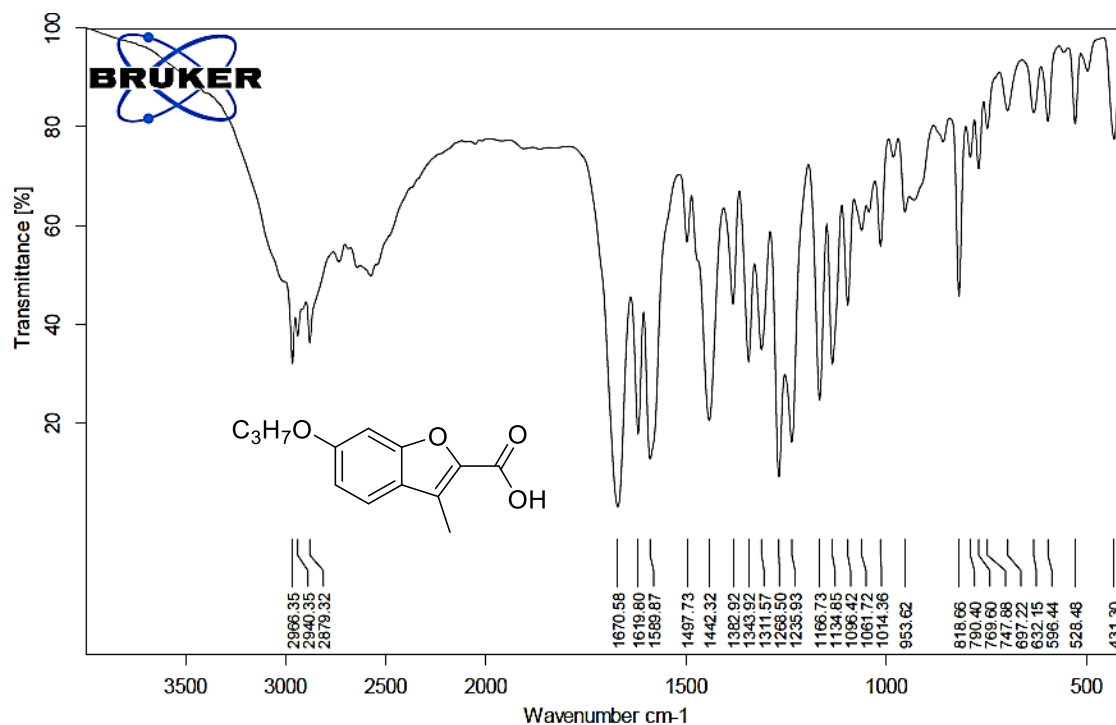
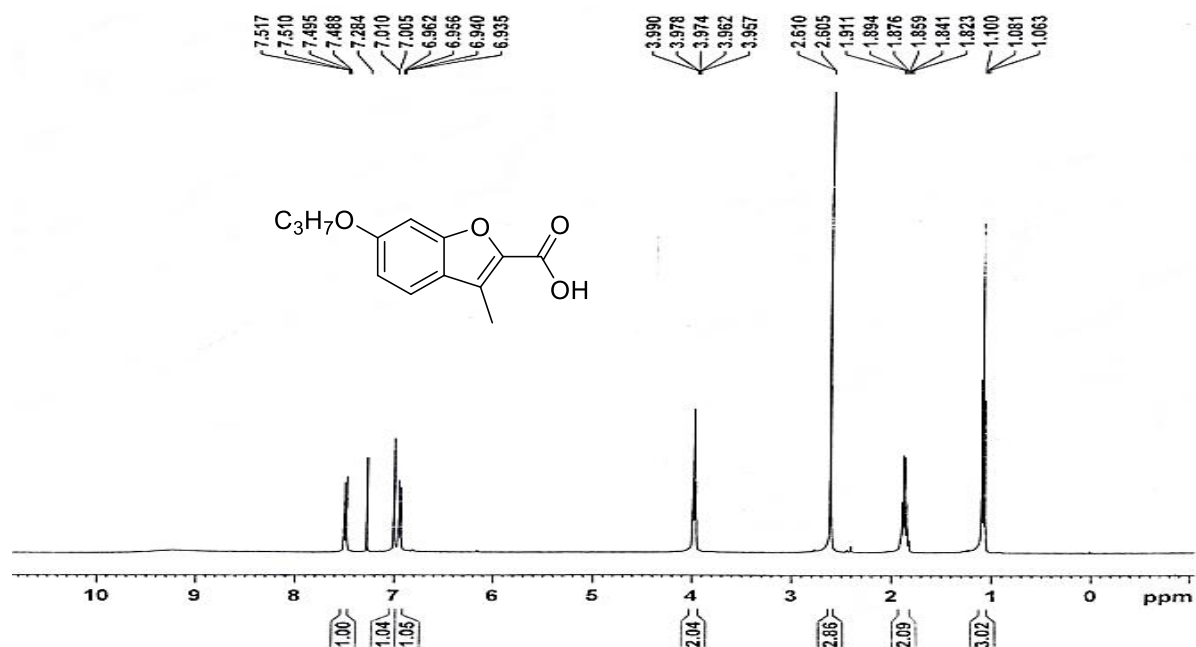
Figure- 2.3.2 ¹H-NMR of 3-methyl-6-propoxybenzofuran-2-carboxylic acid (8)

Figure- 2.4.1 IR of (3-methyl-6-propoxybenzofuran-2-yl)(4-(phenylsulfonyl)piperazin-1-yl) methanone (10a)

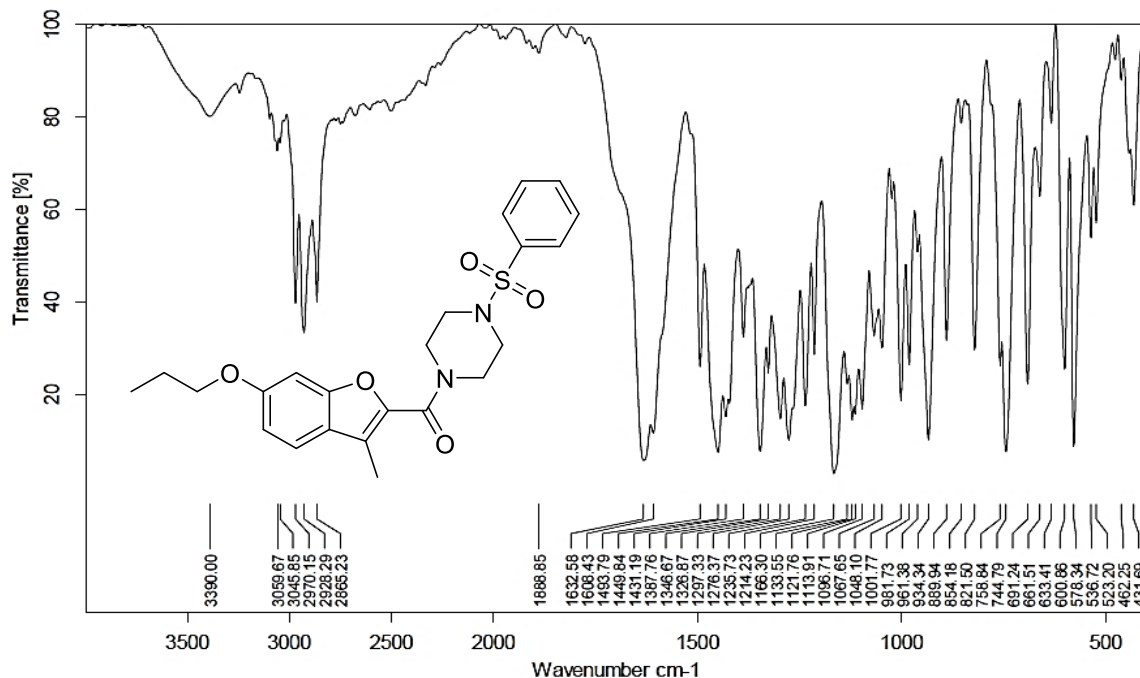


Figure- 2.4.2 $^1\text{H-NMR}$ of (3-methyl-6-propoxybenzofuran-2-yl)(4-(phenylsulfonyl)piperazin-1-yl) methanone (10a)

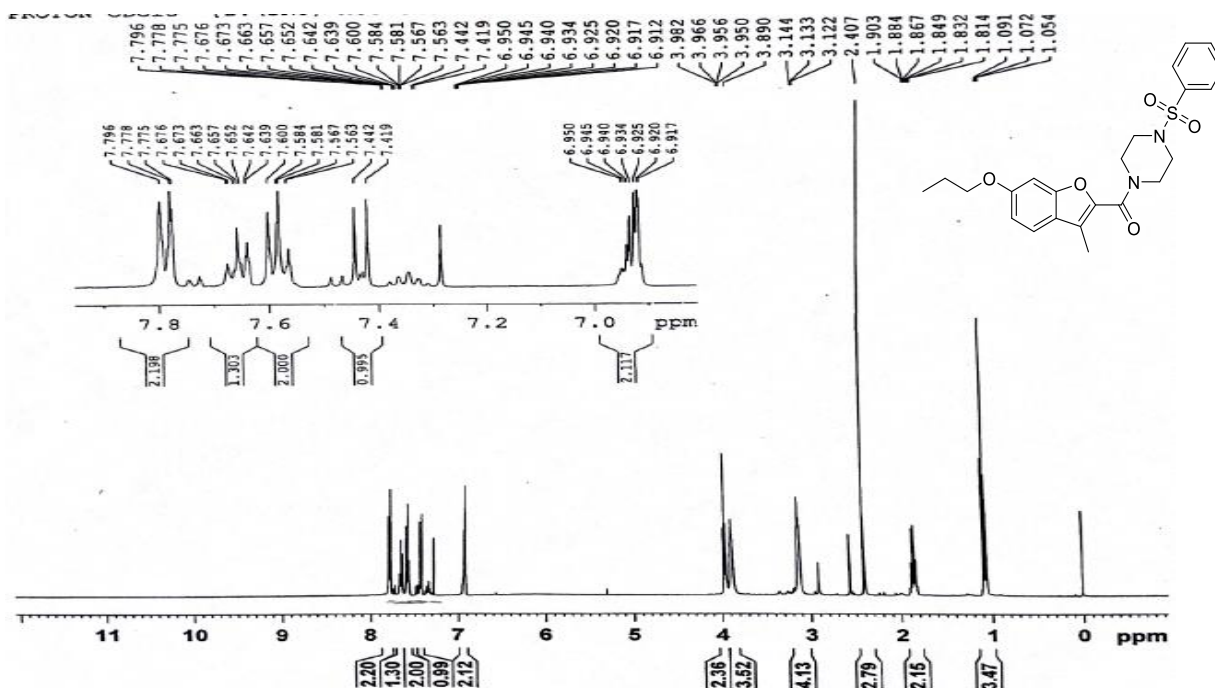


Figure- 2.4.3 ^{13}C -NMR of (3-methyl-6-propoxybenzofuran-2-yl) (4-(phenylsulfonyl) piperazin-1-yl) methanone (**10a**)

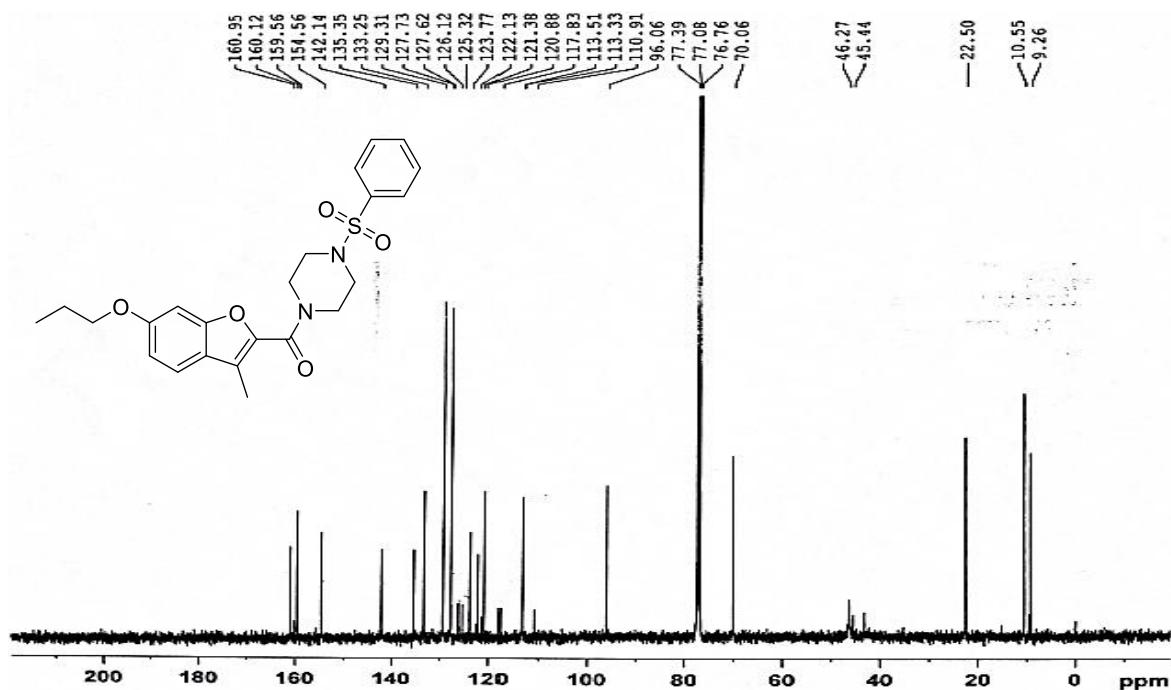


Figure- 2.4.4 Mass of (3-methyl-6-propoxybenzofuran-2-yl) (4-(phenylsulfonyl)piperazin-1-yl)methanone (**10a**) M^+ peak at 442.95

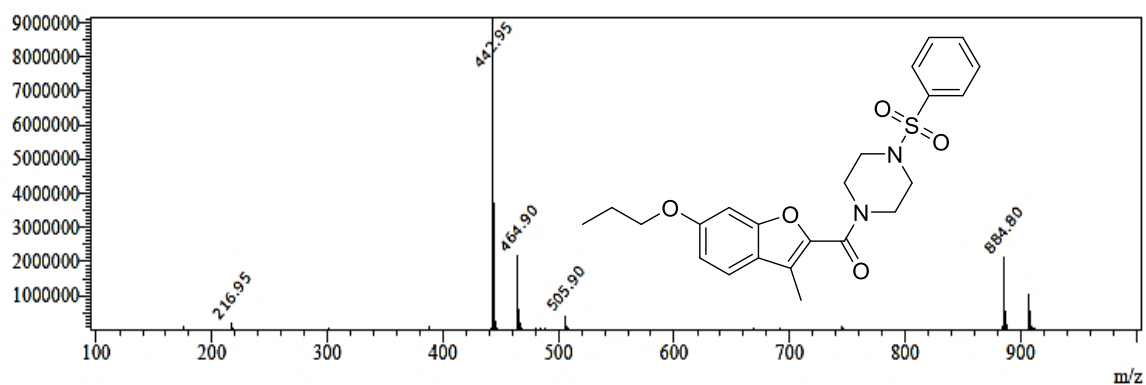


Figure- 2.5.1 IR of (3-methyl-6-propoxybenzofuran-2-yl) (4-tosylpiperazin-1-yl)methanone (**10b**)

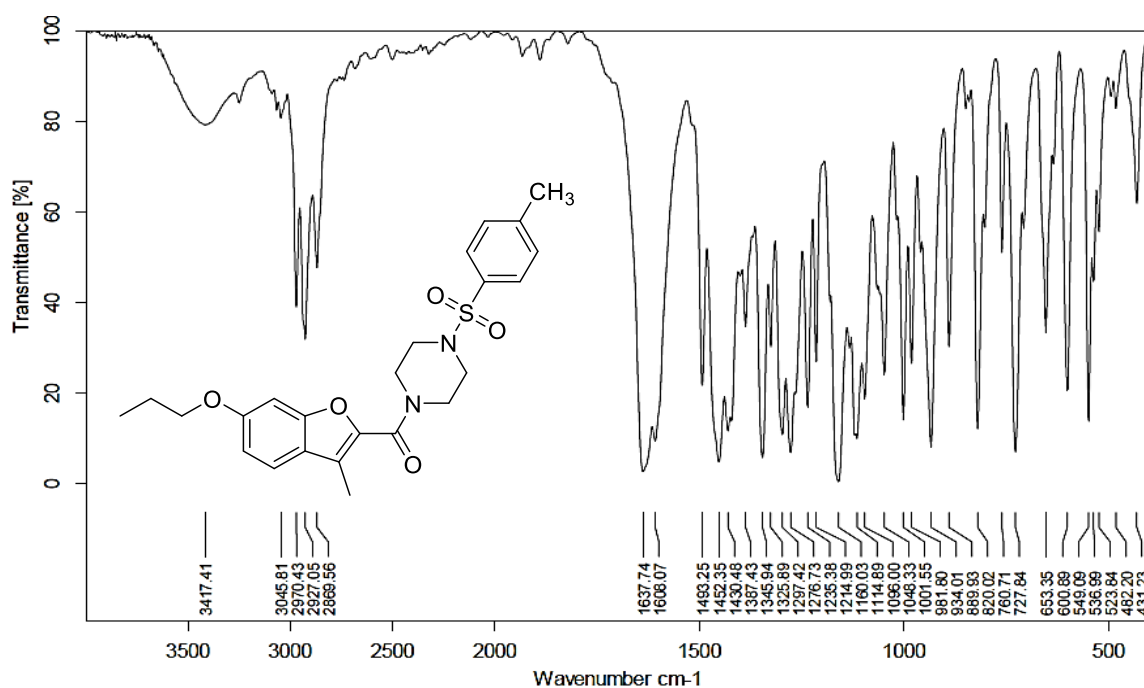


Figure- 2.5.2 $^1\text{H-NMR}$ of (3-methyl-6-propoxybenzofuran-2-yl)(4-tosylpiperazin-1-yl) methanone (**10b**)

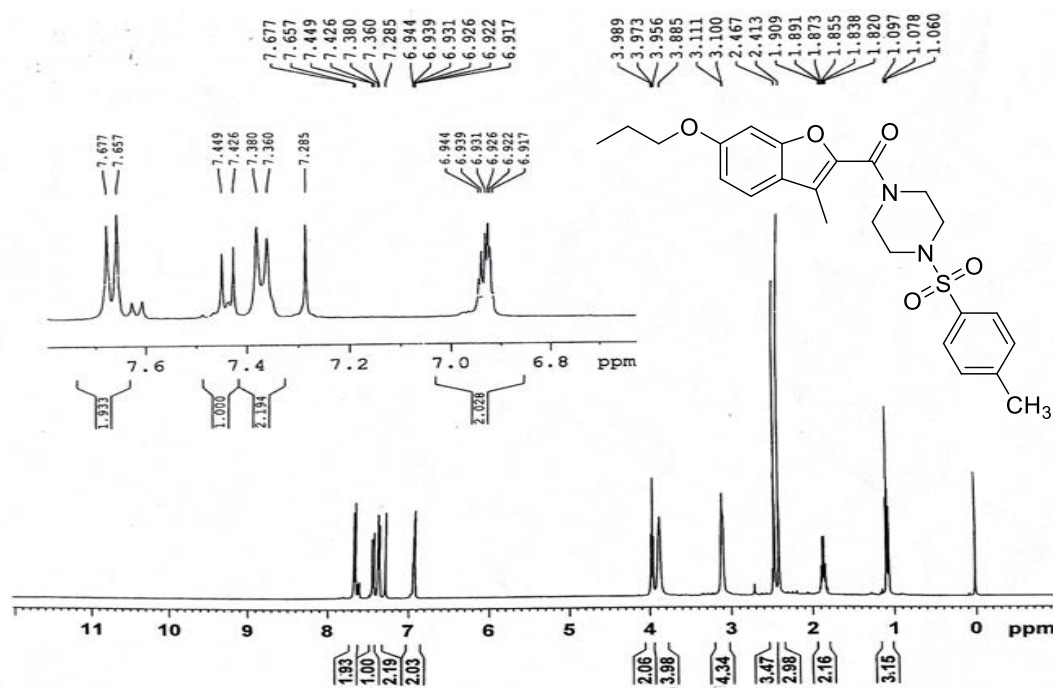


Figure- 2.5.3 ^{13}C -NMR of (3-methyl-6-propoxybenzofuran-2-yl)(4-tosylpiperazin-1-yl)methanone (**10b**)

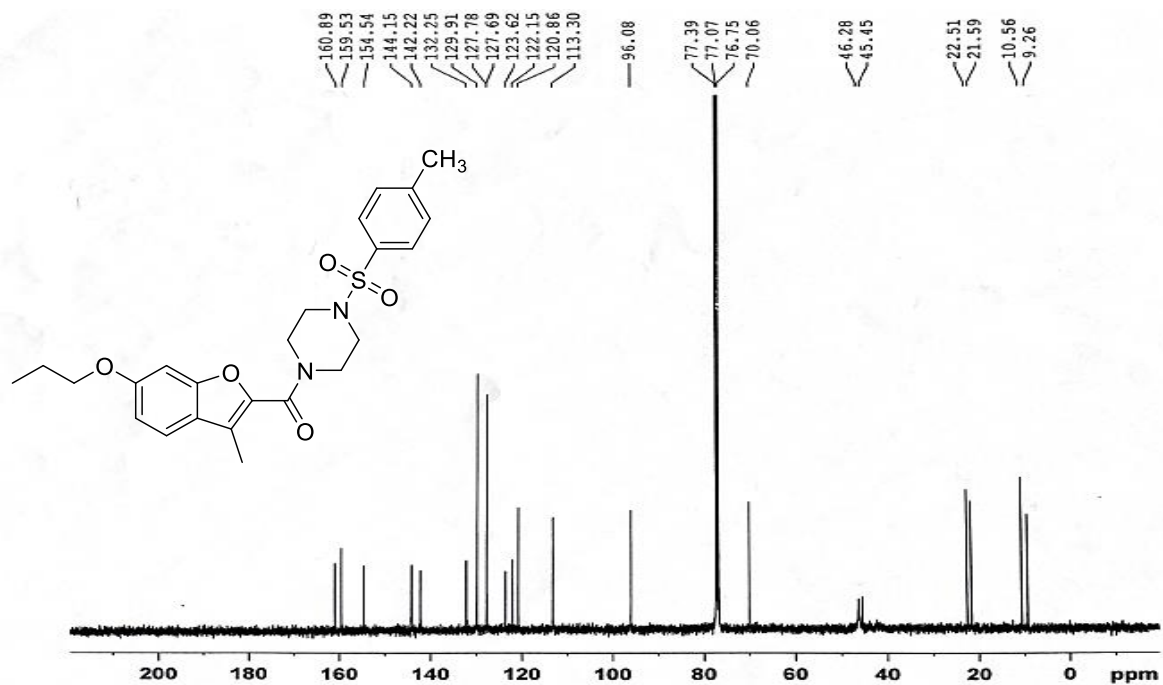


Figure- 2.5.4 Mass of (3-methyl-6-propoxybenzofuran-2-yl)(4-tosylpiperazin-1-yl)methanone (**10b**) M+H peak at 457.10

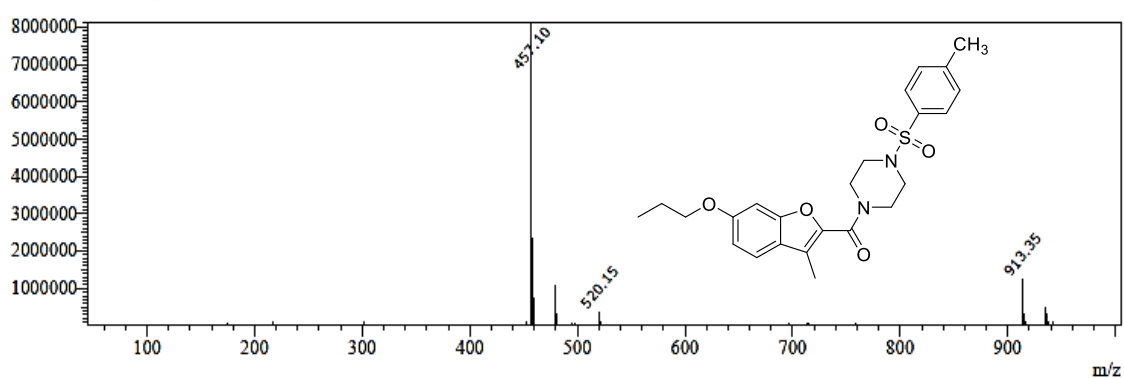


Figure- 2.6.1 IR of (4-((4-chlorophenyl)sulfonyl)piperazin-1-yl)(3-methylbenzofuran-2-yl)methanone (**10c**)

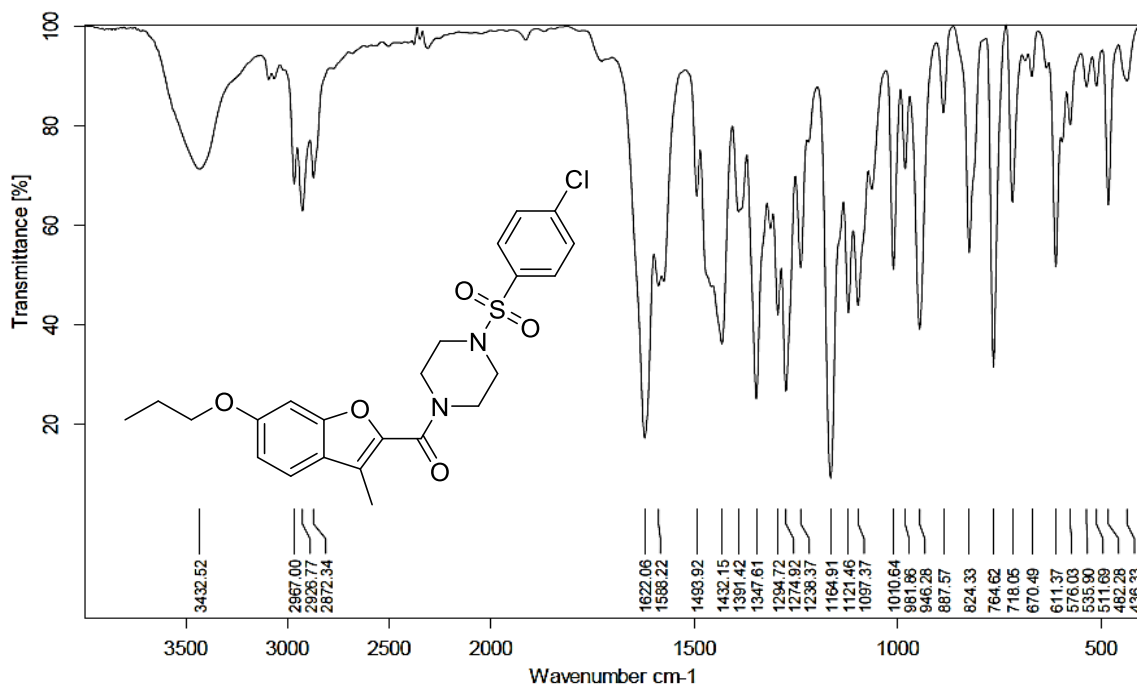


Figure- 2.6.2 ¹H-NMR of (4-((4-chlorophenyl)sulfonyl)piperazin-1-yl)(3-methylbenzofuran-2-yl)methanone (**10c**)

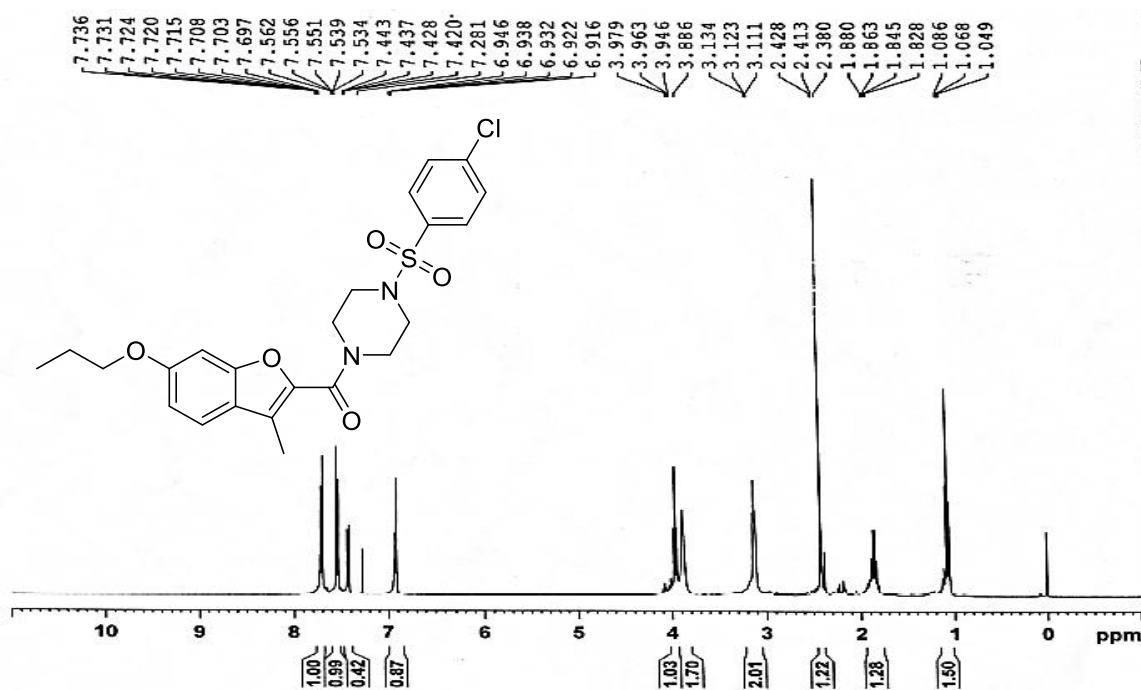


Figure- 2.6.3 ^{13}C -NMR of (4-((4-chlorophenyl)sulfonyl)piperazin-1-yl)(3-methylbenzofuran-2-yl)methanone (**10c**)

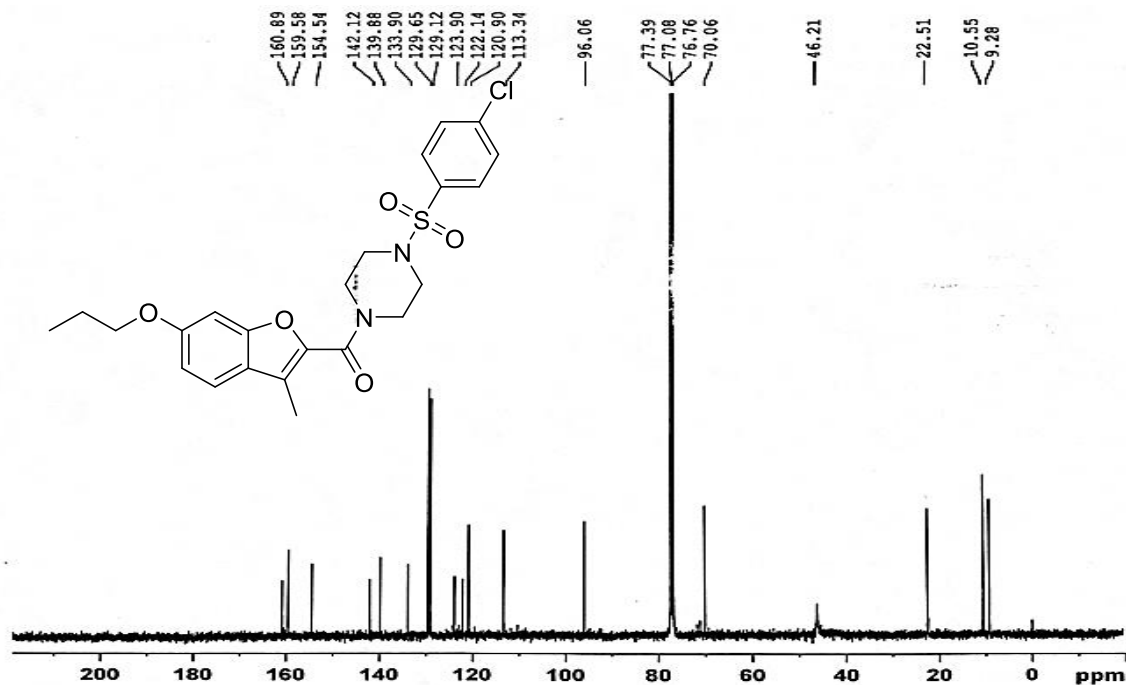


Figure- 2.6.4 Mass of (4-((4-chlorophenyl)sulfonyl)piperazin-1-yl)(3-methylbenzofuran-2-yl)methanone (**10c**) M+H peak at 477.05

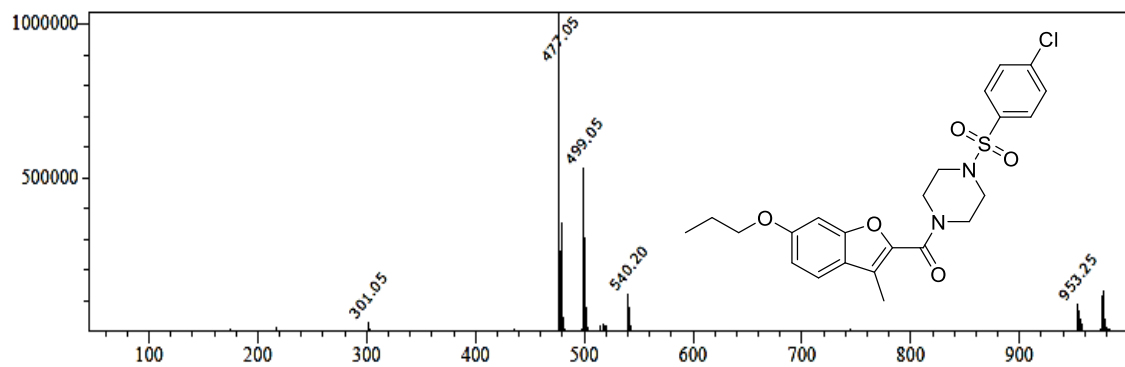


Figure- 2.7.3 ^{13}C -NMR of (4-((4-Bromophenyl)sulfonyl)piperazin-1-yl)(3-methylbenzofuran-2-yl)methanone (**10d**)

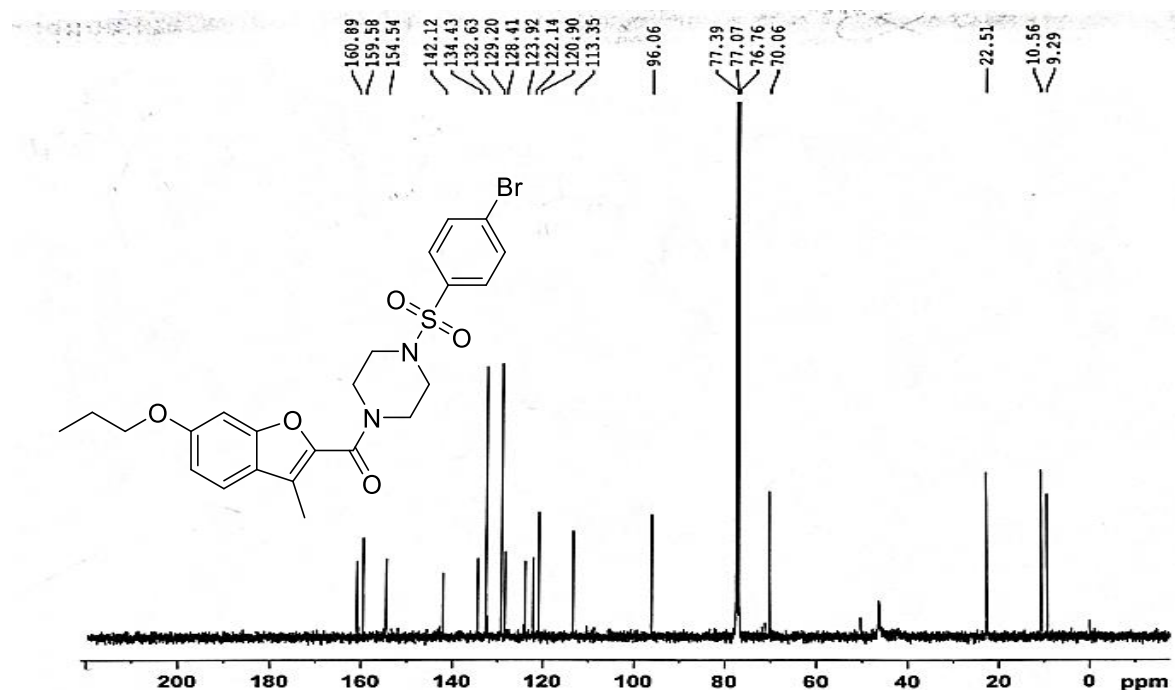


Figure- 2.7.4 Mass of (4-((4-Bromophenyl)sulfonyl)piperazin-1-yl) (3-methylbenzofuran-2-yl)methanone (**10d**) M+H peak at 523.00

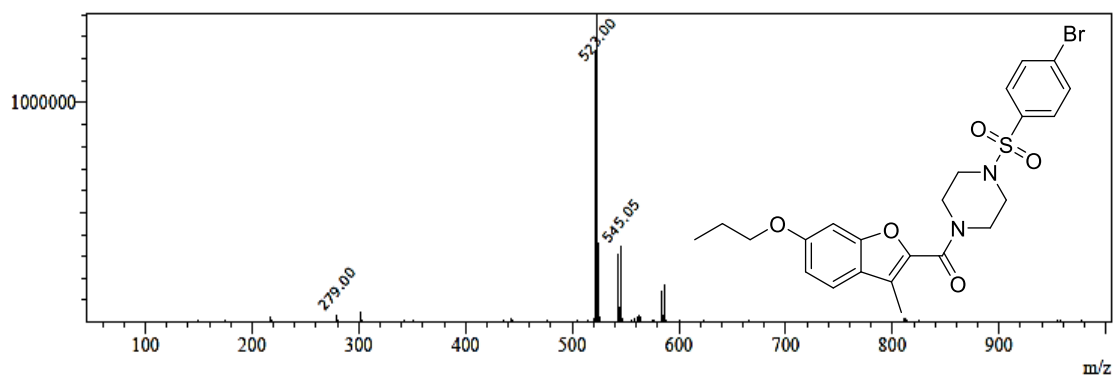


Figure- 2.8.1 IR of (3-methyl-6-propoxybenzofuran-2-yl)(4-(nitrophenyl)sulfonyl) piperazin-1-yl)methanone (**10e**)

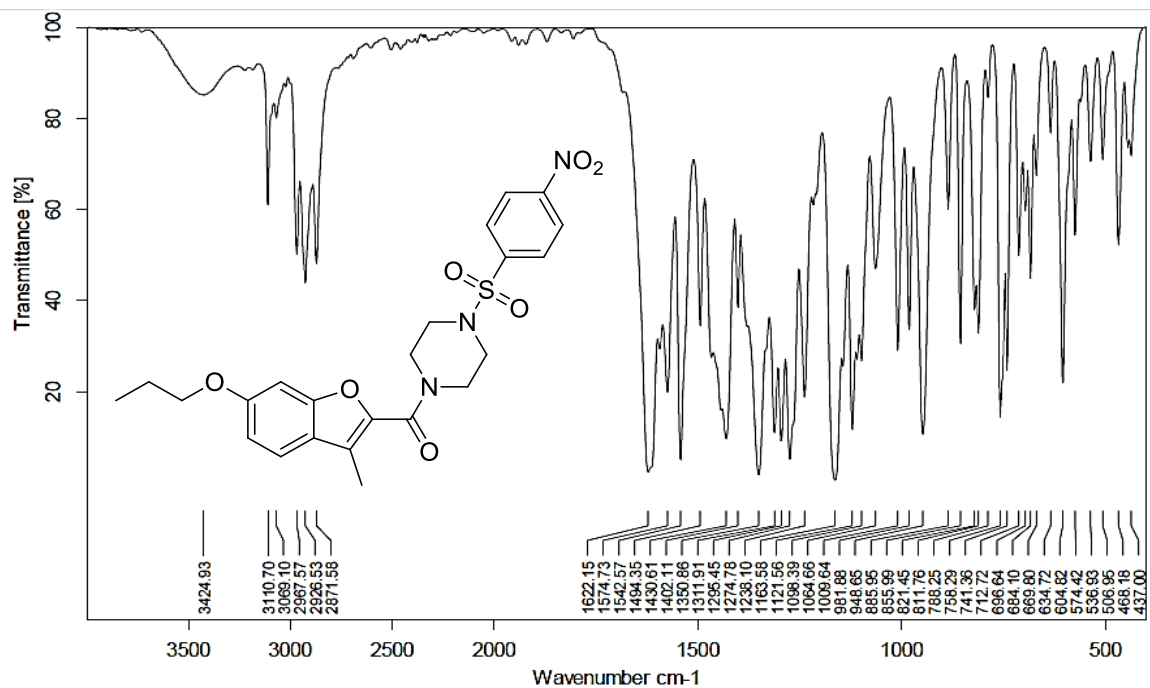


Figure- 2.8.2 $^1\text{H-NMR}$ of (3-methyl-6-propoxybenzofuran-2-yl)(4-(nitrophenyl)sulfonyl) piperazin-1-yl)methanone (**10e**)

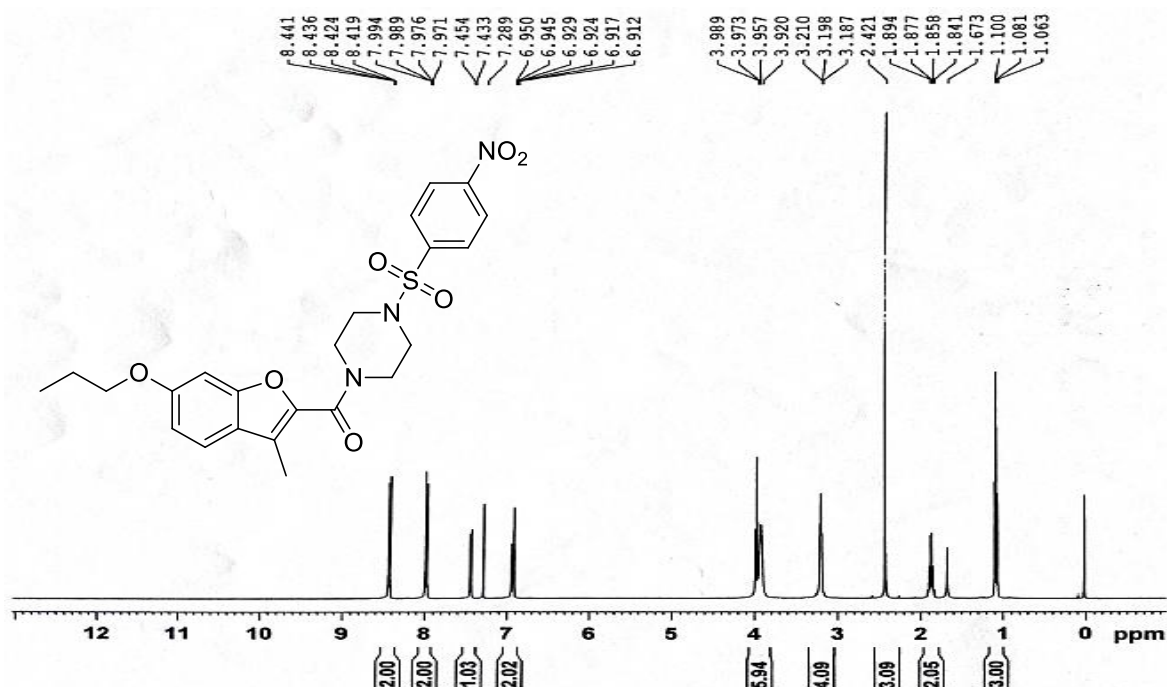


Figure- 2.8.3 ^{13}C -NMR of (3-Methyl-6-propoxybenzofuran-2-yl)(4-(nitrophenyl)sulfonyl) piperazin-1-yl)methanone (**10e**)

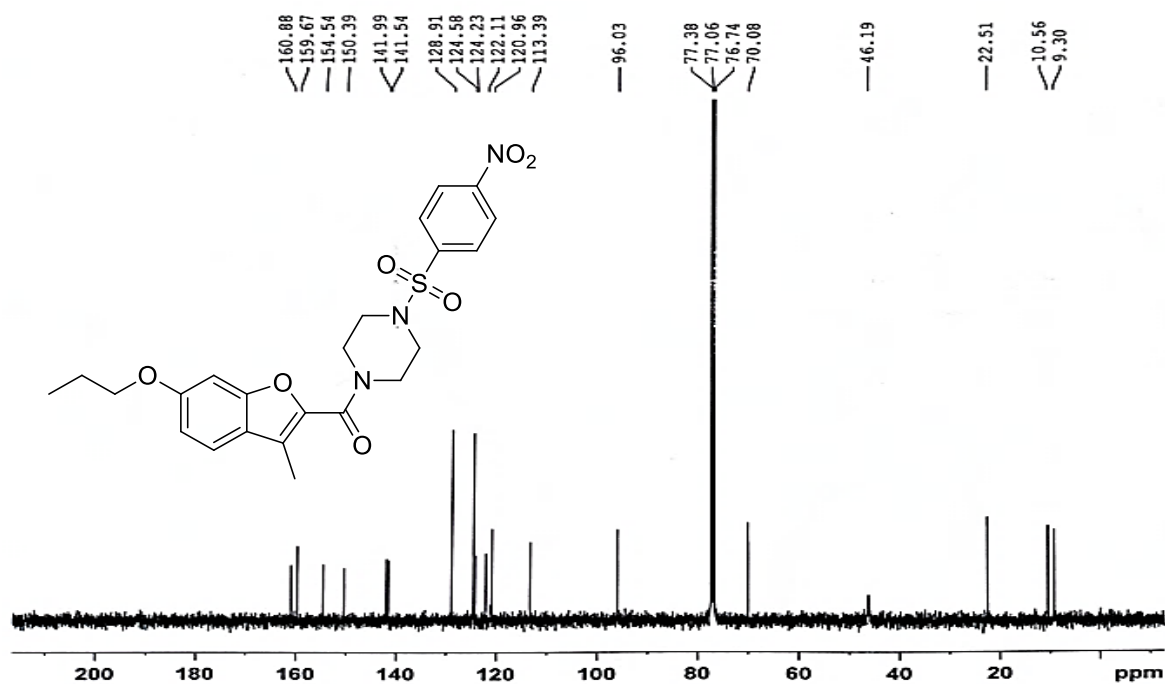


Figure- 2.8.4 Mass of (3-methyl-6-propoxybenzofuran-2-yl)(4-(nitrophenyl)sulfonyl) piperazin-1-yl)methanone (**10e**) M^+ peak at 487.70

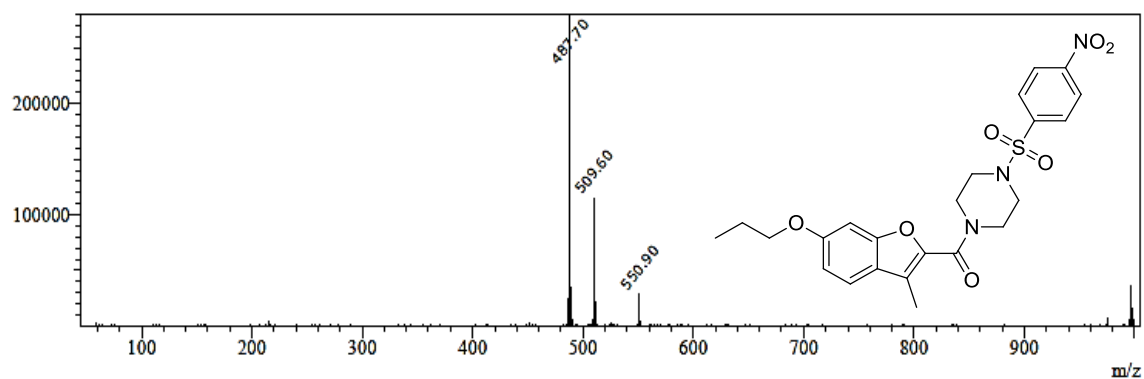


Figure- 2.9.1 IR of N'-Benzoyl-3-methyl-6-propoxybenzofuran-2-carbohydrazide (12a)

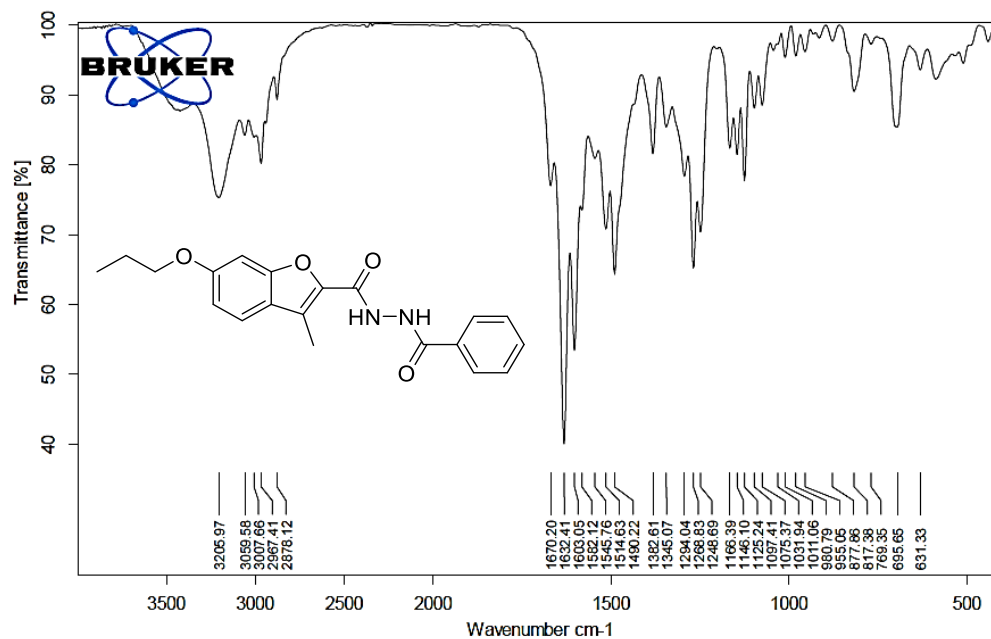
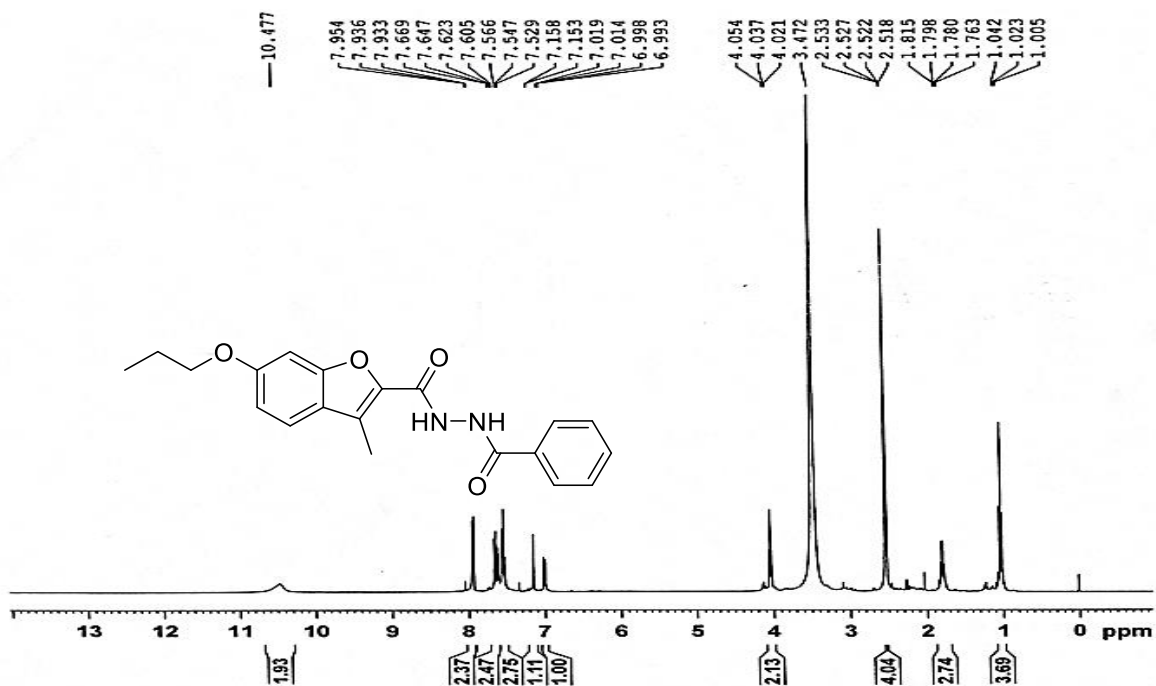
Figure- 2.9.2 ¹H-NMR of N'-Benzoyl-3-methyl-6-propoxybenzofuran-2-carbohydrazide (12a)

Figure- 2.9.3 ^{13}C -NMR of N'-Benzoyl-3-methyl-6-propoxybenzofuran-2-carbohydrazide (12a)

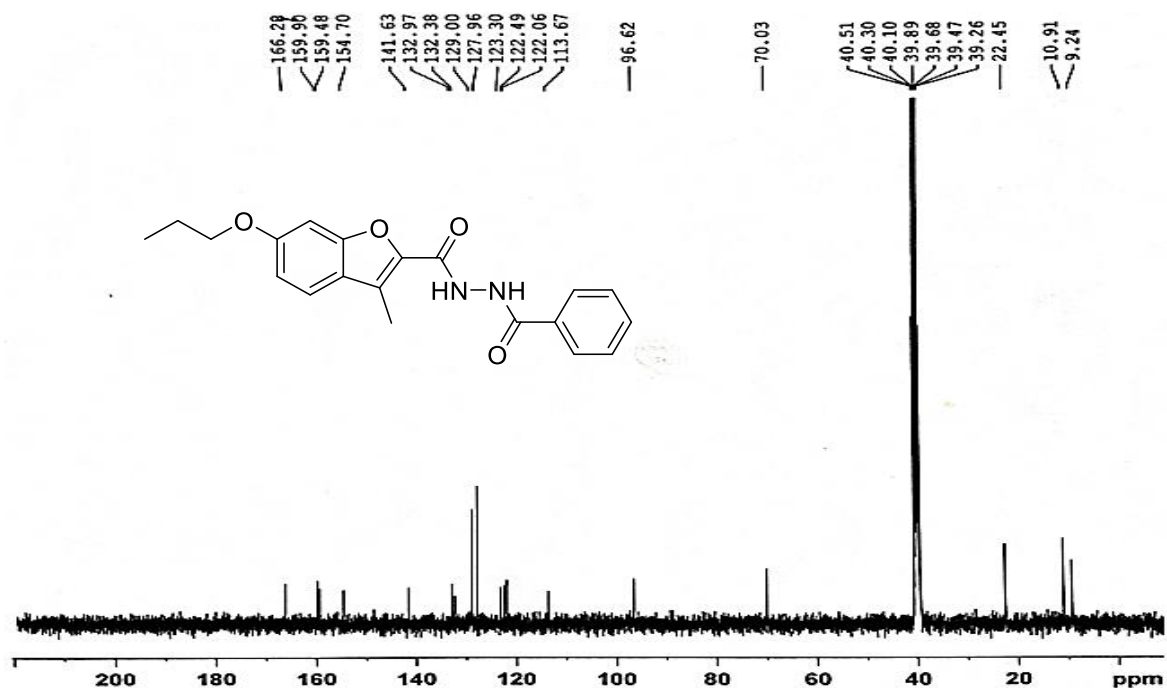


Figure- 2.9.4 Mass of N'-Benzoyl-3-methyl-6-propoxybenzofuran-2-carbohydrazide (12a)
M+H peak at 353.00

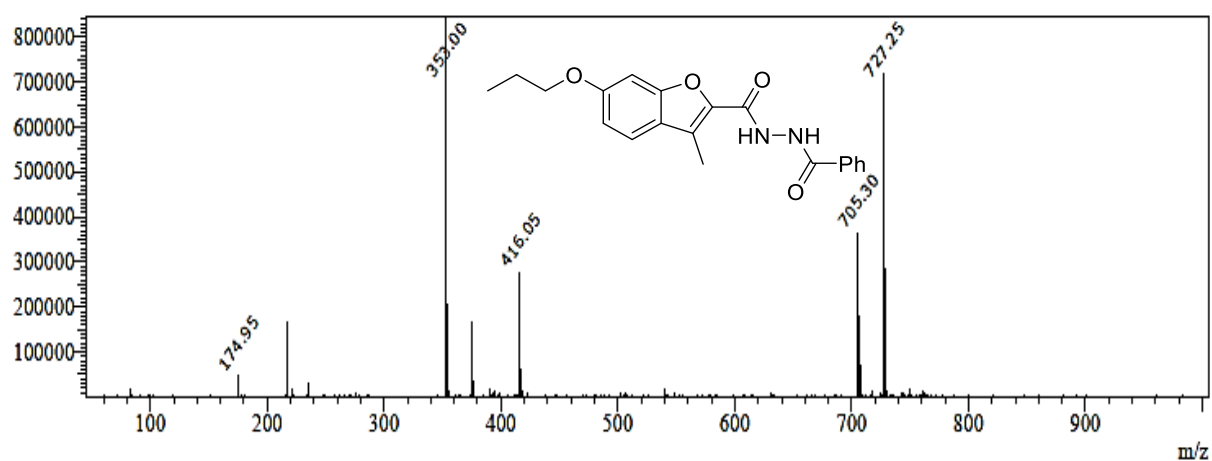


Figure- 2.10.1 IR of N'-(4-Chlorobenzoyl)-3-methyl-6-propoxybenzofuran-2-carbohydrazide (12b)

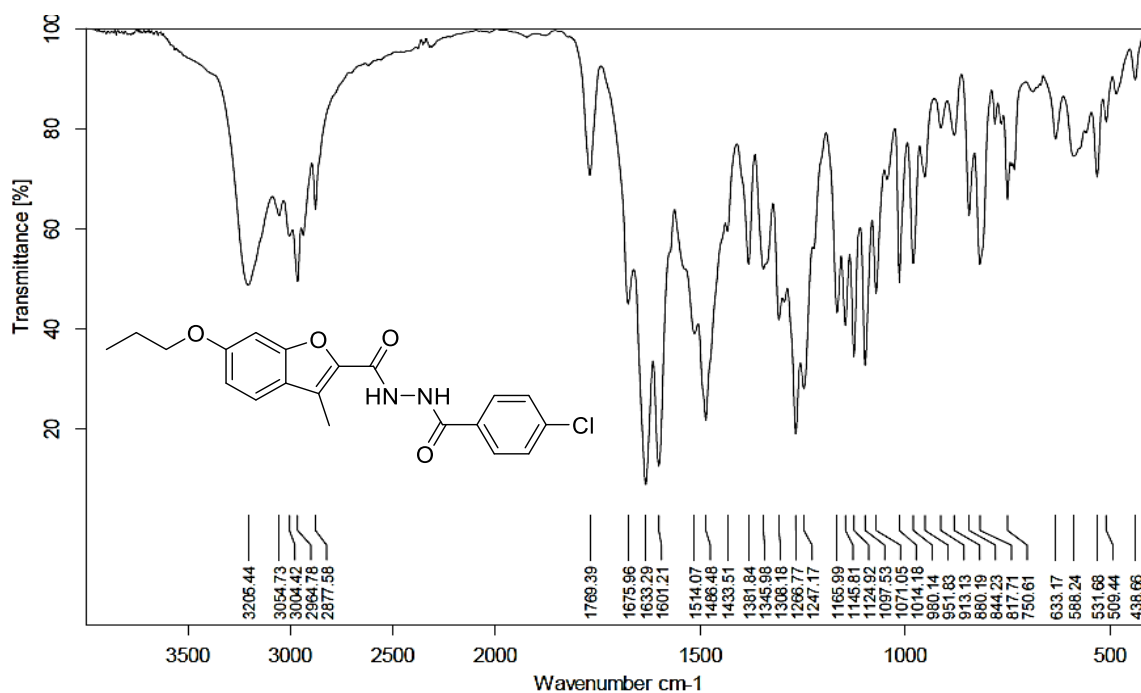


Figure- 2.10.2 ¹H-NMR of N'-(4-Chlorobenzoyl)-3-methyl-6-propoxybenzofuran-2-carbohydrazide (12b)

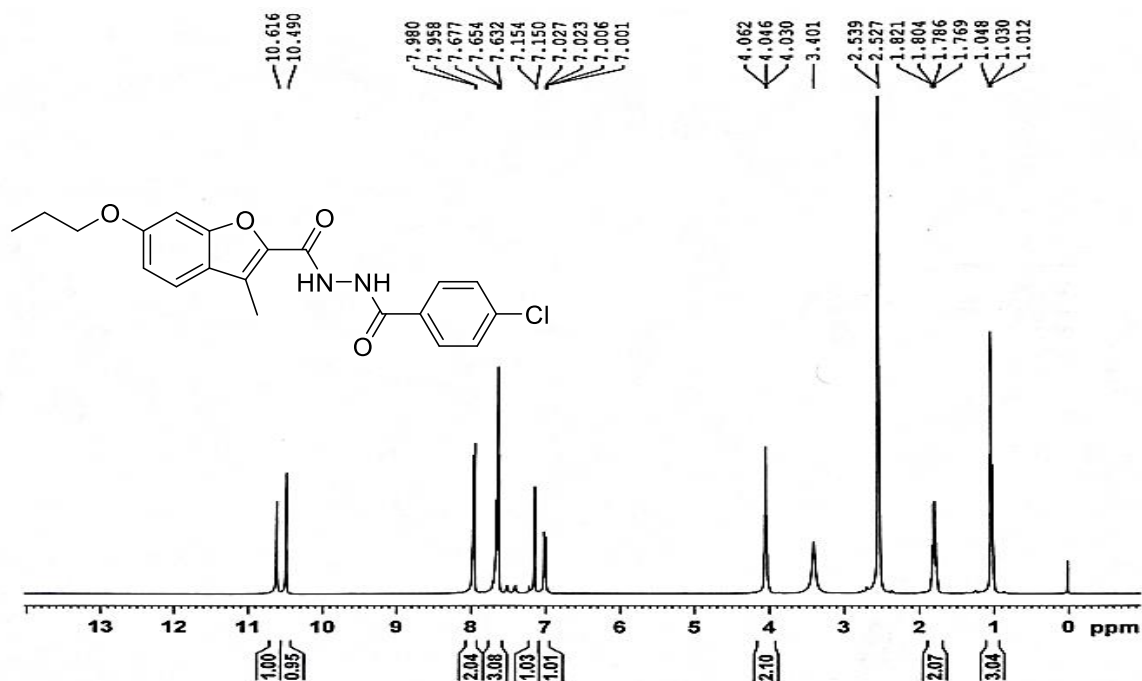


Figure- 2.10.3 ^{13}C -NMR of N'-(4-Chlorobenzoyl)-3-methyl-6-propoxybenzofuran-2-carbohydrazide (**12b**)

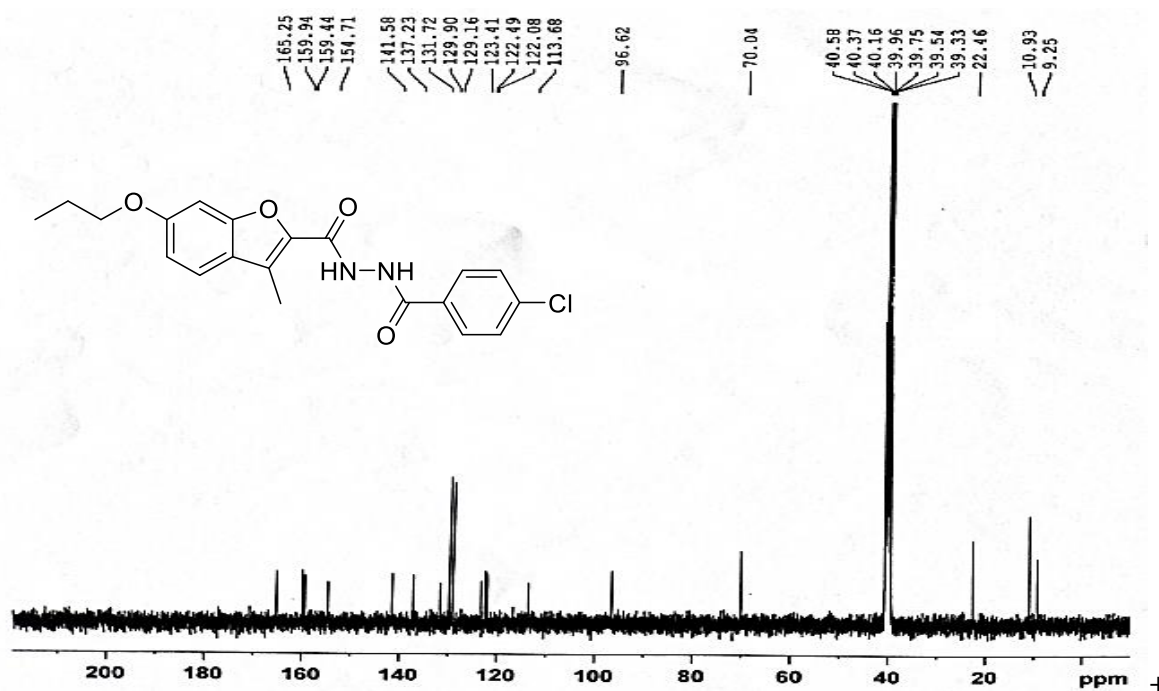


Figure- 2.10.4 Mass of N'-(4-Chlorobenzoyl)-3-methyl-6-propoxybenzofuran-2-carbohydrazide (**12b**) M^+ peak at 386.60

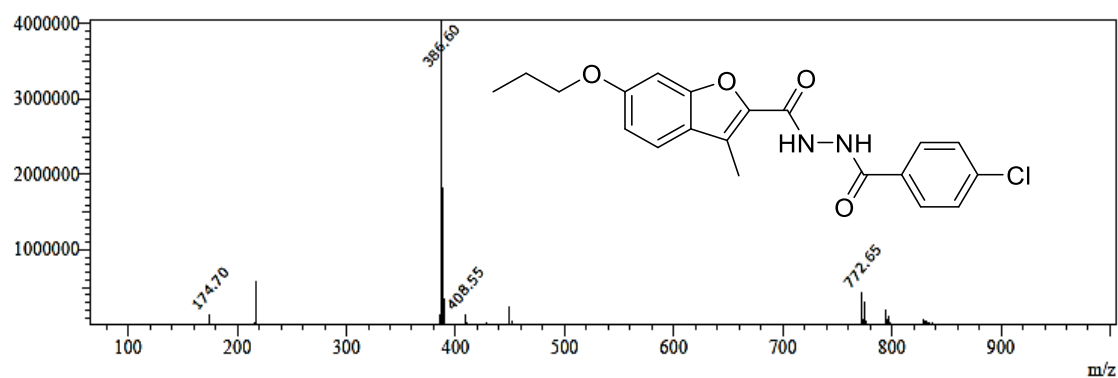


Figure- 2.11.1 IR of 3-methyl-N'-(3-nitrobenzoyl)-6-propoxybenzofuran-2-carbohydrazide (12c)

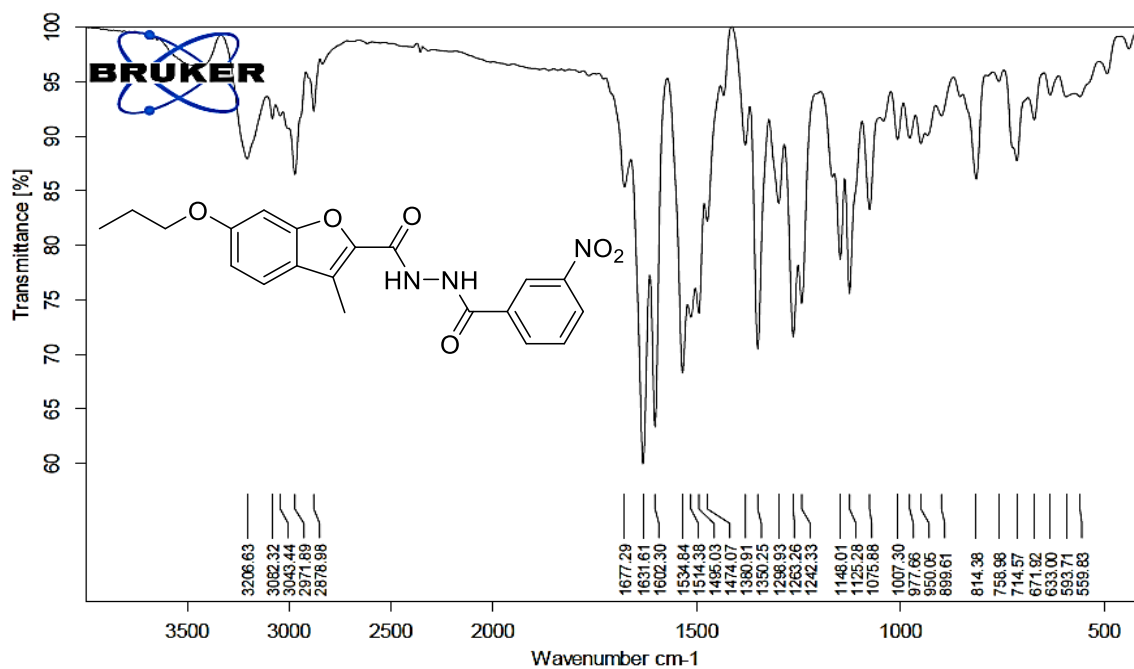


Figure- 2.11.2 ¹H-NMR of 3-methyl-N'-(3-nitrobenzoyl)-6-propoxybenzofuran-2-carbohydrazide (12c)

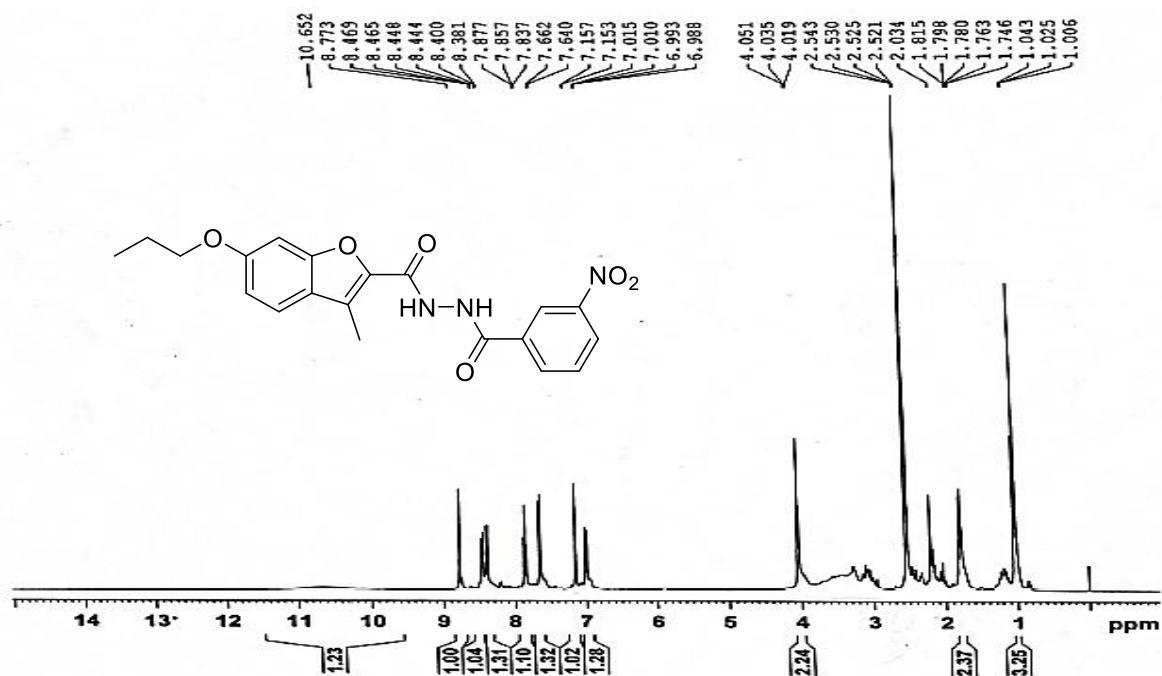


Figure- 2.11.3 ^{13}C -NMR of 3-methyl-N'-(3-nitrobenzoyl)-6-propoxybenzofuran-2-carbohydrazide (**12c**)

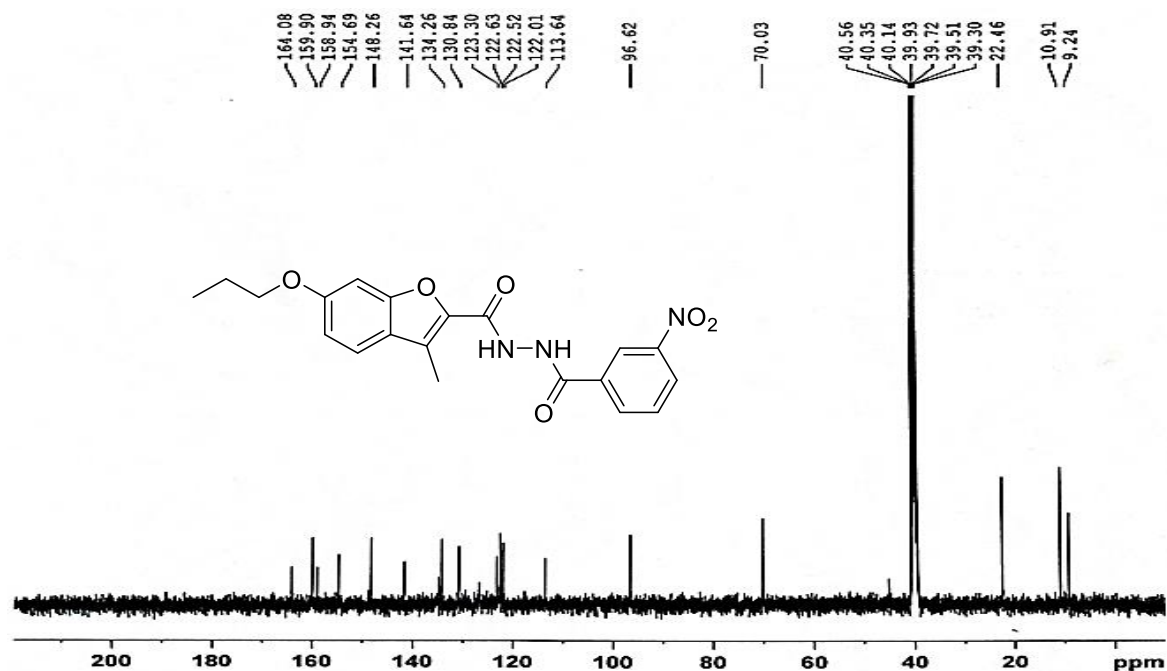


Figure- 2.11.4 Mass of 3-methyl-N'-(3-nitrobenzoyl)-6-propoxybenzofuran-2-carbohydrazide (**12c**) M^+ peak at 397.90

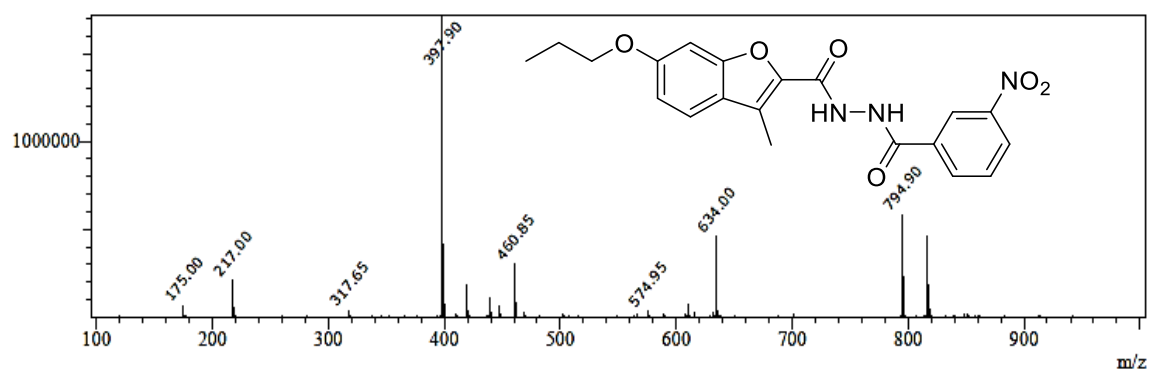


Figure- 2.12.1 IR of N'-(3-Methyl-6-propoxybenzofuran-2-carbonyl)isonicotinohydrazide (12d)

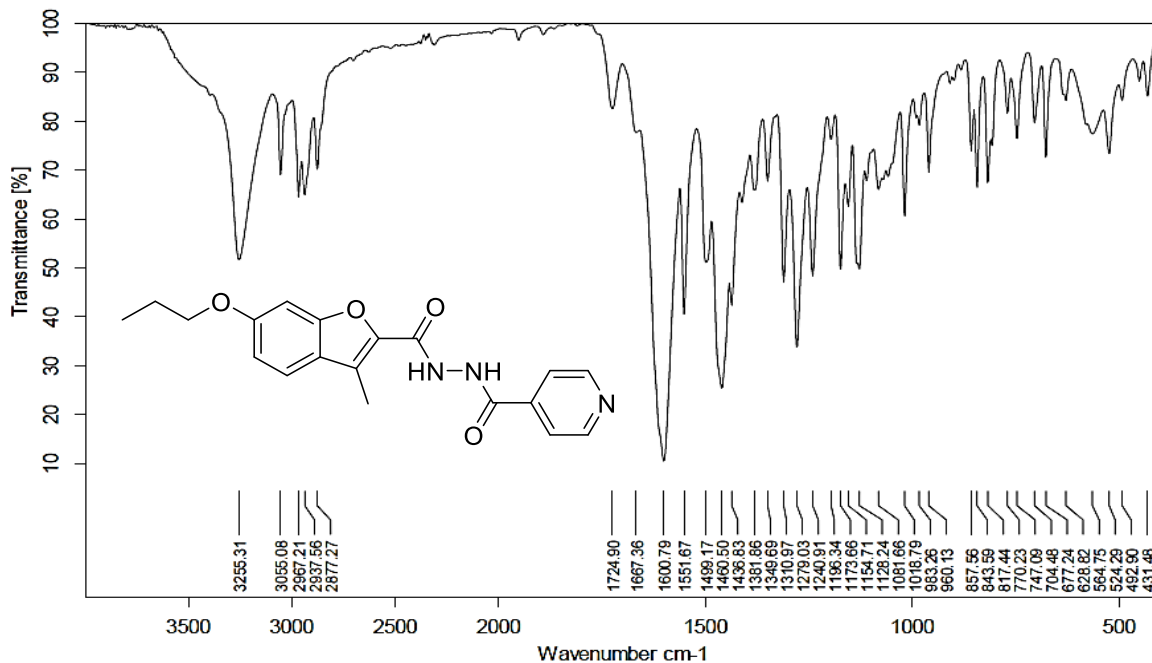


Figure- 2.12.2 $^1\text{H-NMR}$ N'-(3-Methyl-6-propoxybenzofuran-2-carbonyl)isonicotinohydrazide (12d)

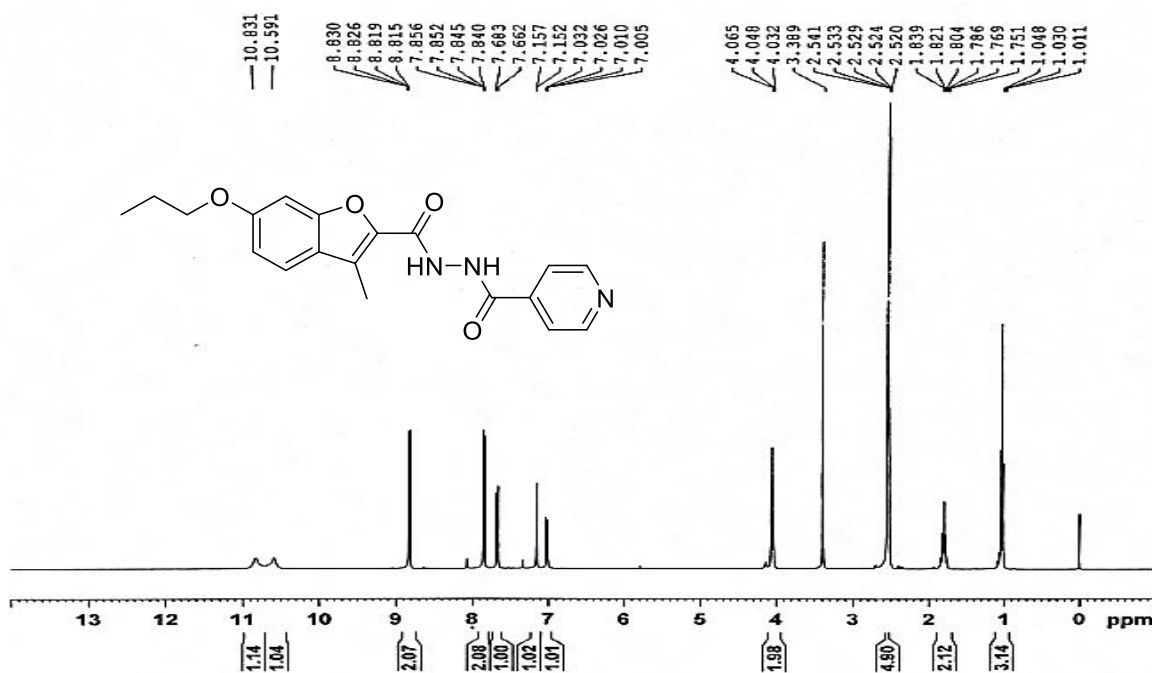


Figure- 2.12.3 ^{13}C -NMR of N'-(3-Methyl-6-propoxybenzofuran-2-carbonyl) isonicotinohydrazide (**12d**)

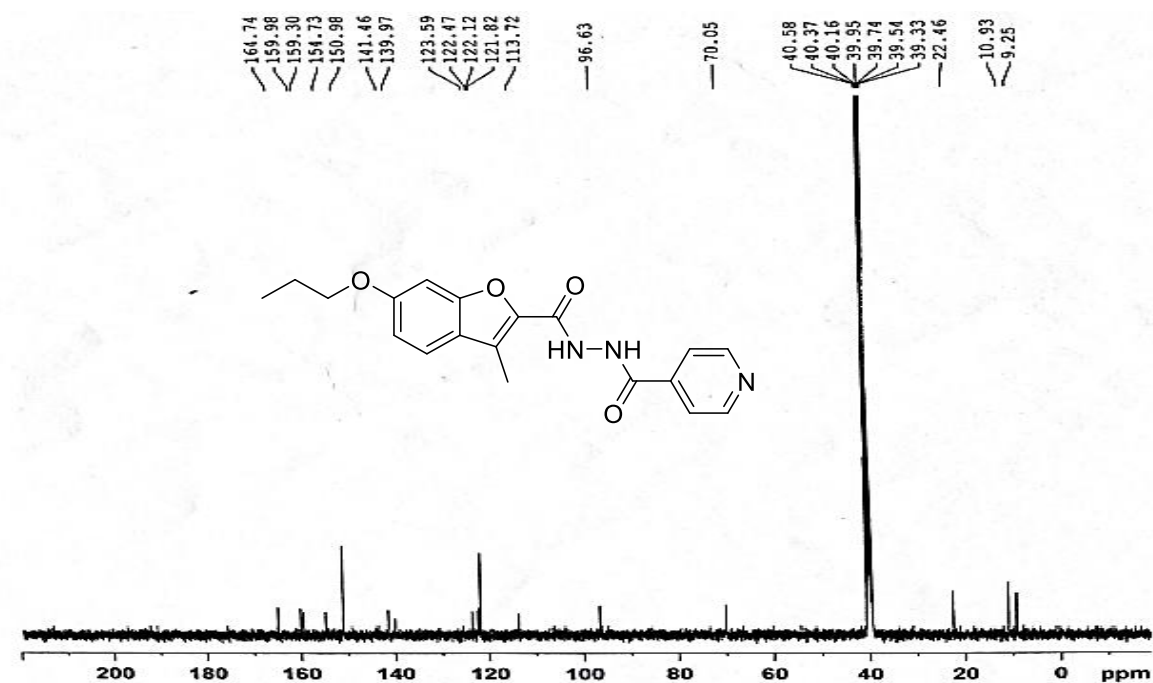


Figure- 2.12.4 Mass of N'-(3-Methyl-6-propoxybenzofuran-2-carbonyl)isonicotinohydrazide (**12d**) M+H peak at 354.05

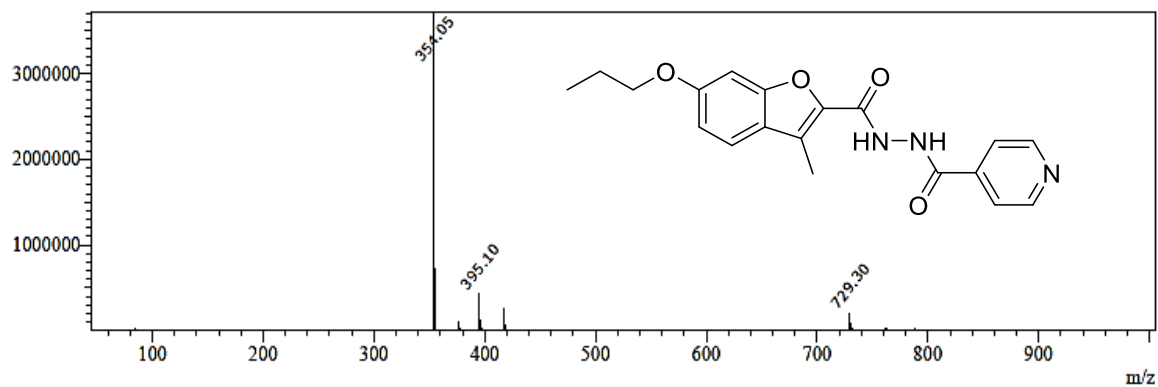


Figure- 2.13.1 IR of 3-Methyl-N'-phenyl-6-propoxybenzofuran-2-carbohydrazide (14a)

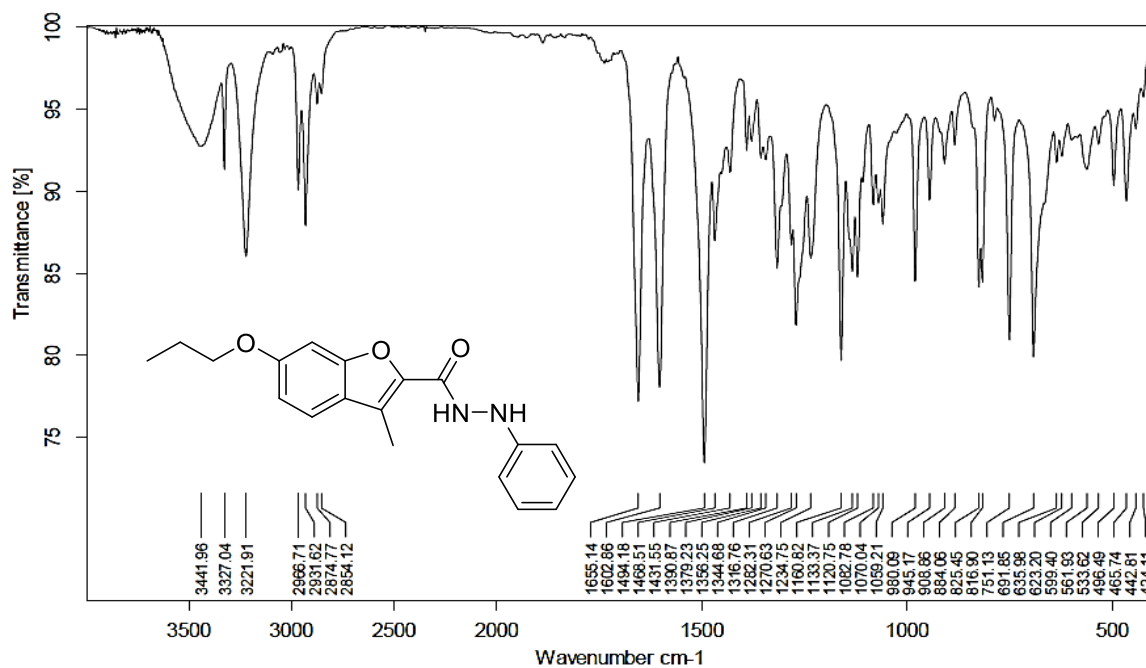
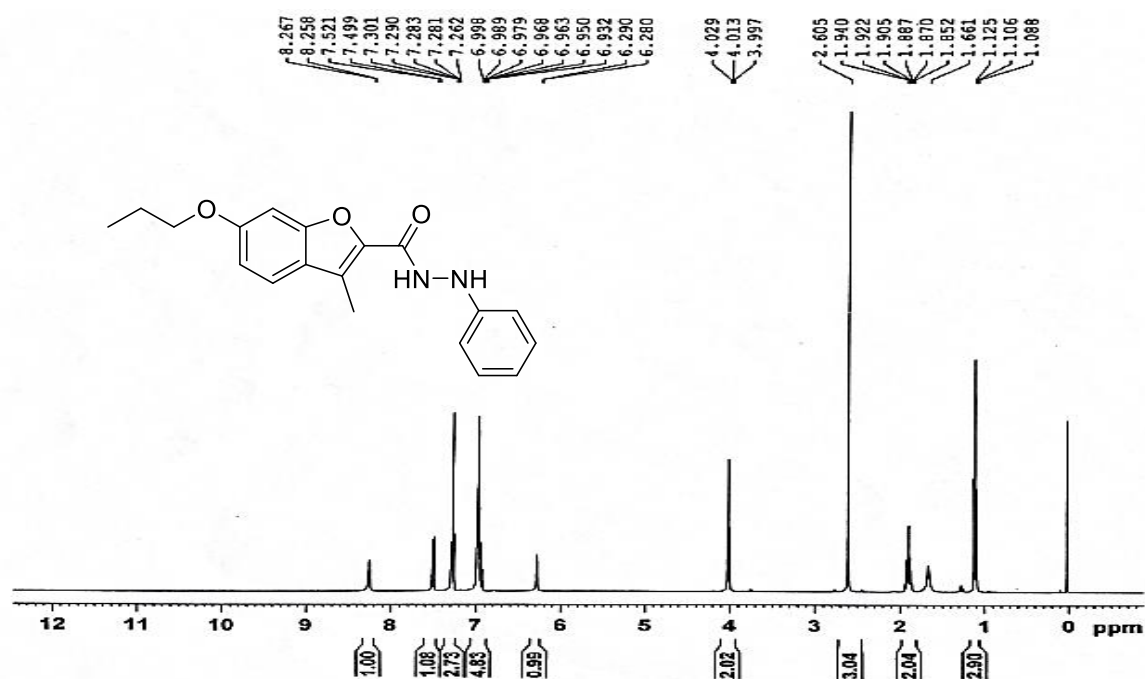
Figure- 2.13.2 ¹H-NMR of 3-Methyl-N'-phenyl-6-propoxybenzofuran-2-carbohydrazide (14a)

Figure- 2.13.3 ^{13}C -NMR of 3-Methyl-N'-phenyl-6-propoxybenzofuran-2-carbohydrazide (14a)

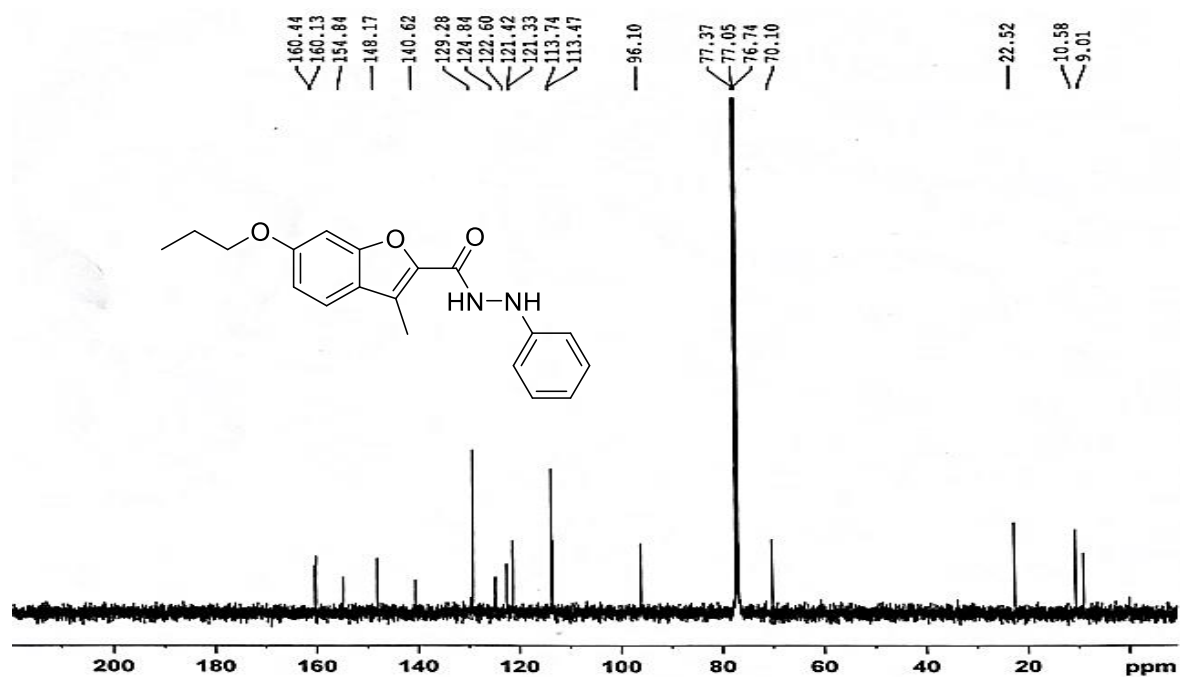


Figure- 2.13.4 Mass of 3-Methyl-N'-phenyl-6-propoxybenzofuran-2-carbohydrazide(14a)
M+H peak at 324.90

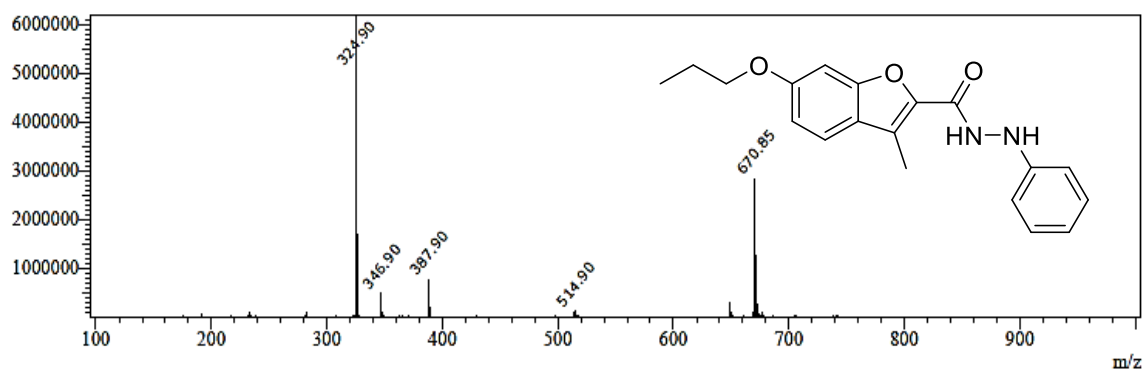


Figure- 2.14.1 IR NMR of N'-(4-Chlorophenyl)-3-methyl-6-propoxybenzofuran-2-carbohydrazide (**14b**)

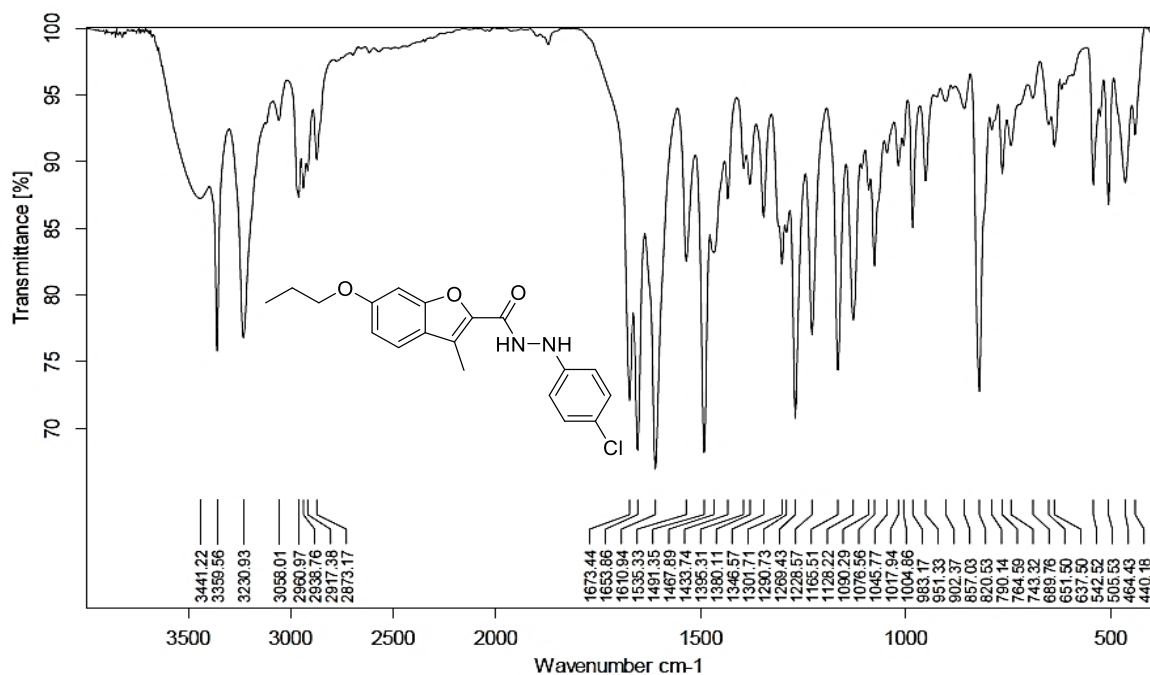


Figure- 2.14.2 ¹H-NMR of N'-(4-Chlorophenyl)-3-methyl-6-propoxybenzofuran-2-carbohydrazide (**14b**)

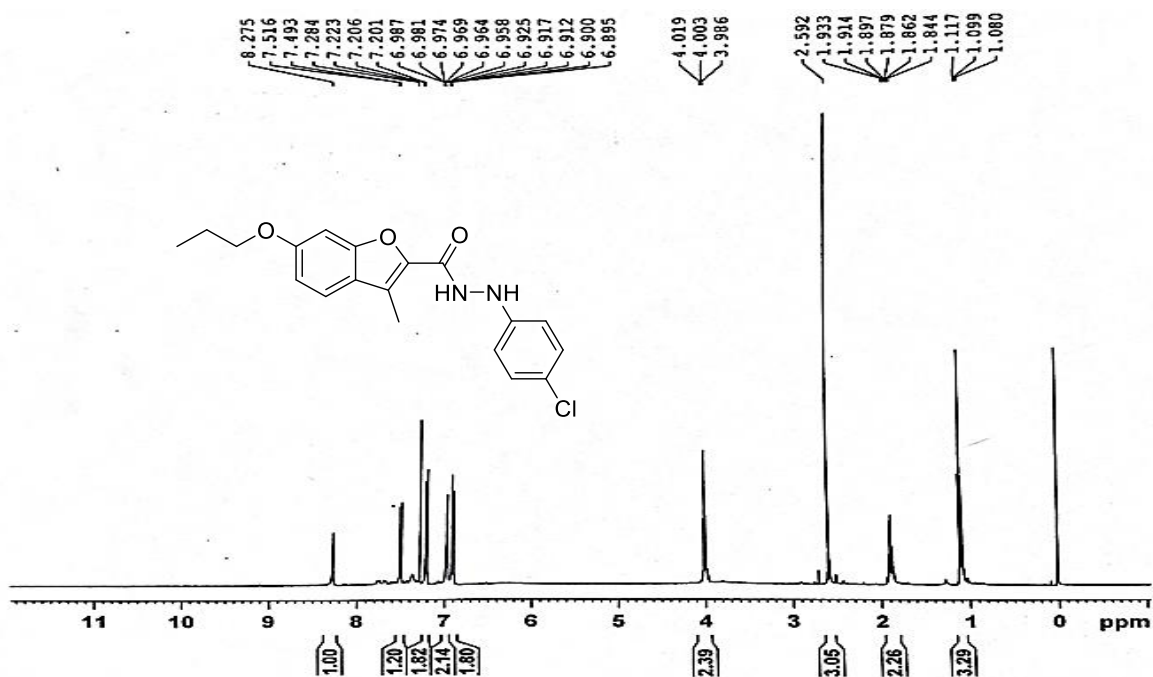


Figure- 2.14.3 ^{13}C -NMR of N'-(4-Chlorophenyl)-3-methyl-6-propoxybenzofuran-2-carbohydrazide (**14b**)

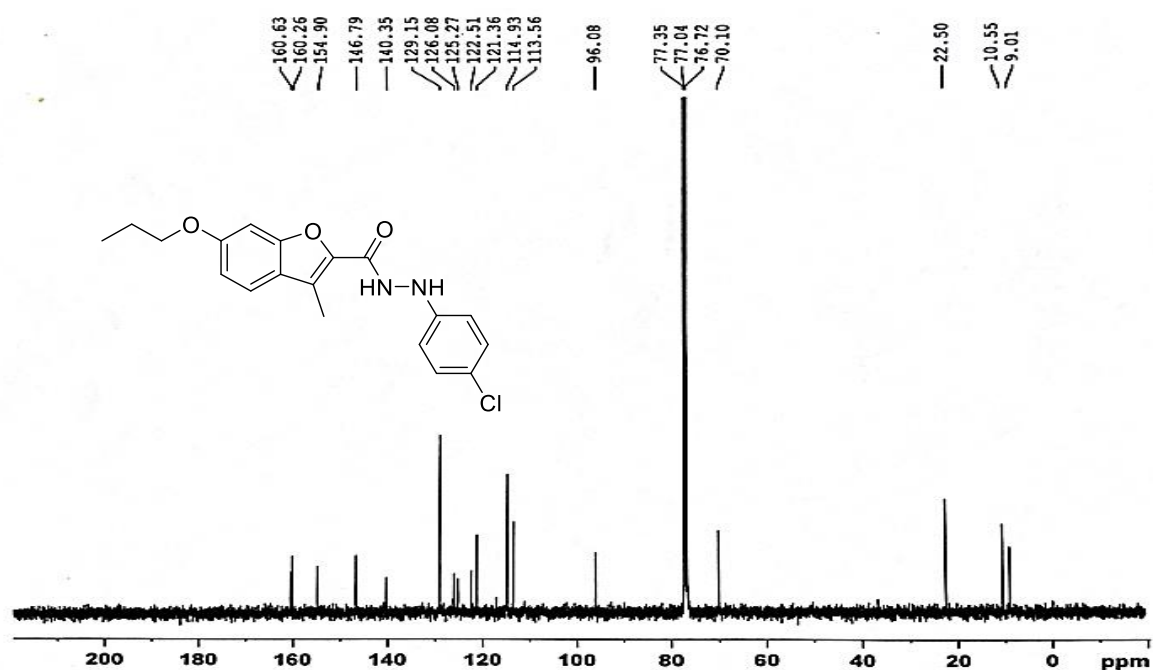


Figure- 2.14.4 Mass N'-(4-Chlorophenyl)-3-methyl-6-propoxybenzofuran-2-carbohydrazide (**14b**) M^+ peak at 358.90

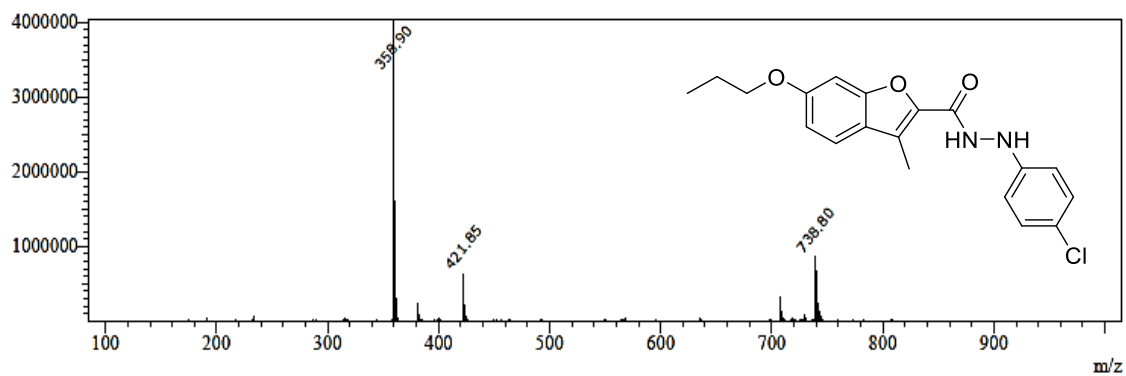


Figure- 2.15.1 IR of N'-(2,4-Dichlorophenyl)-3-methyl-6-propoxybenzofuran-2-carbohydrazide (**14c**)

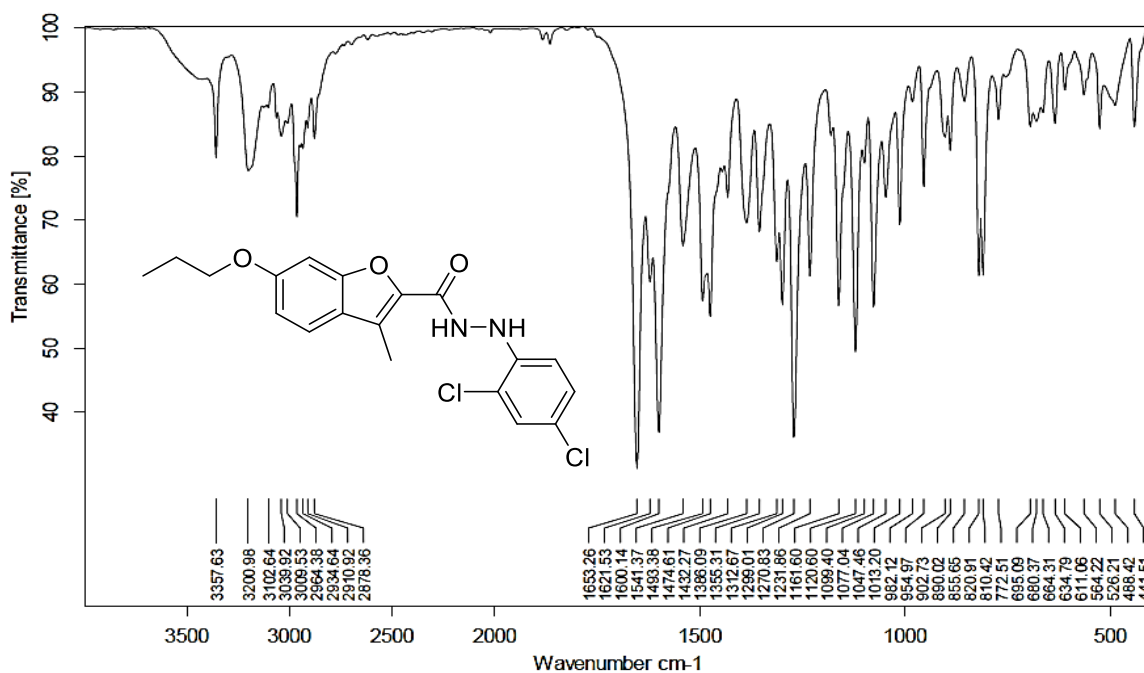


Figure- 2.15.2 $^1\text{H-NMR}$ of N'-(2,4-Dichlorophenyl)-3-methyl-6-propoxybenzofuran-2-carbohydrazide (**14c**)

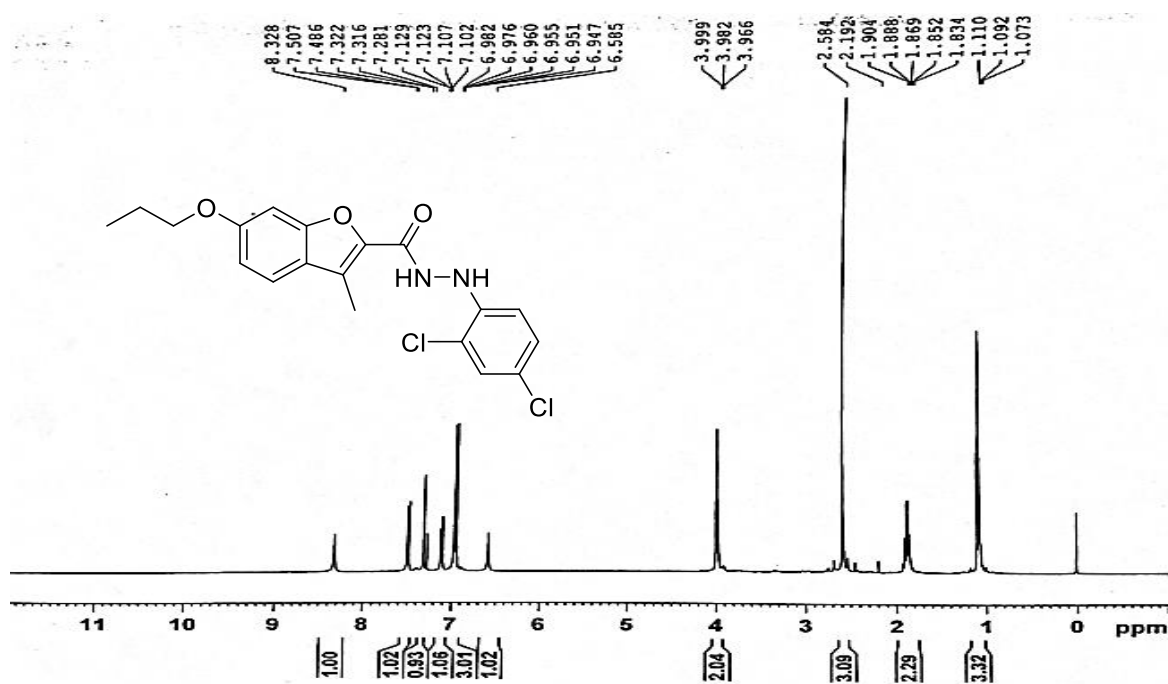


Figure- 2.15.3 ^{13}C -NMR of N'-(2,4-Dichlorophenyl)-3-methyl-6-propoxybenzofuran-2-carbohydrazide (**14c**)

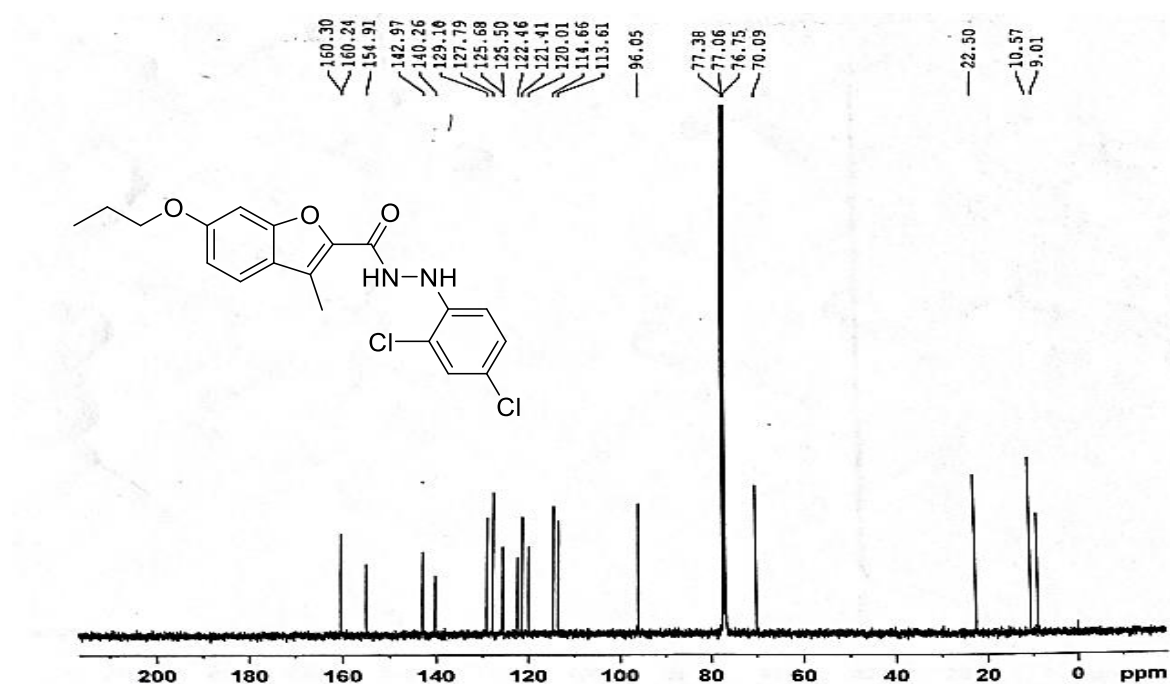
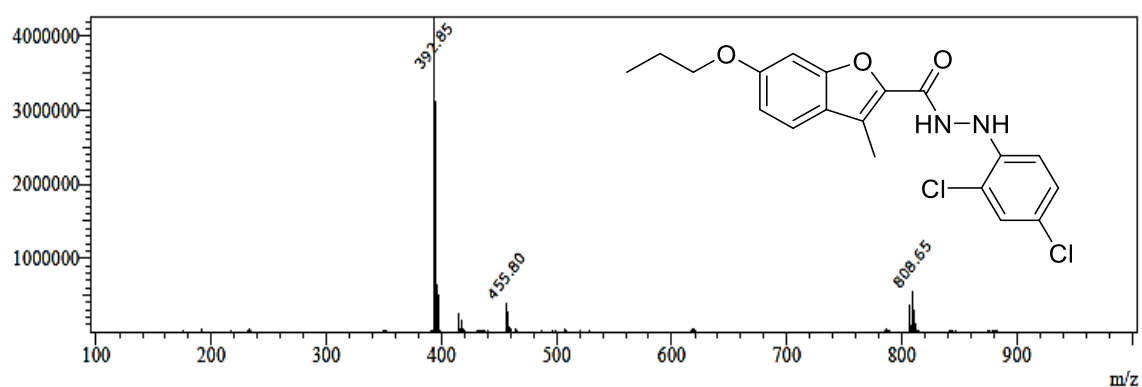


Figure- 2.15.4 Mass of N'-(2,4-Dichlorophenyl)-3-methyl-6-propoxybenzofuran-2-carbohydrazide (**14c**) M^+ peak at 392.85



2.2.2 Biological Evaluation

2.2.3 Structure activity relationship (SAR) for Anticancer activity by MTT assay:

Benzofuran carboxamide derivatives **10a-e**, **12a-d** and **14a-c** were screened for their anticancer activity against A549 (Lungs cancer cell line), MCF-7 (Breast cancer cell line) using MTT assay (**Table 2.1**). In benzofuran carboxamide derivatives with arylsulfonamide piperazines, compound **10a** showed poor activity against both tested cell lines. Addition of methyl group on arylsulphonamide piperazine part, compound **10b** showed good activity with IC₅₀ values 3.08±.003 μM and 4.9±.0239 μM against A549 and MCF-7 cell lines respectively.

Table 2.1: Anticancer activity against A549 (Lungs cancer cell line), MCF-7 (Breast cancer cell line) for compounds **10a-e**, **12a-d** and **14a-c**

Compound	IC ₅₀ μM ^a	
	A549	MCF7
10a	16.77±.034	10.22±.045
10b	3.08±.003	4.9±.0239
10c	8.97±.092	2.74±.026
10d	1.504±.056	2.07±0.65
10e	1.04±.006	4.391±.032
12a	16.41±.401	13.45±.25
12b	0.858±.0049	7.756±1.03
12c	9.07±0.21	7.49±.042
12d	22.61±.96	4.86±0.72
14a	3.66±.073	9.34±.019
14b	1.822±.029	4.19±1.27
14c	1.86±.023	23.1±1.02
Fluorouracil	11.13 ±0.083	45.04 ±1.02

^aIC₅₀ values were determined based on MTT assay using GraphPad Prism software.

On replacing methyl group with chloro in compound **10c**, resulted in drop of activity against A549 cell lines, however against MCF-7 activity was found to be better. Bromo analogue compound **10d** showed very good activity against both the cell lines with IC₅₀ values 1.504±.056 μM and 2.07±0.65 μM against A549 and MCF-7 cell lines respectively. On replacing halogen with electron withdrawing group nitro in compound **10e**, resulted in very

good activity against A549 cell line with IC_{50} values $1.04 \pm 0.006 \mu\text{M}$ as compared to standard drug, however anticancer activity was slightly dropped against MCF-7 cell line.

In another variation benzofuran carboxylic acid derivative was reacted with substituted aryl hydrazides to give compounds **12a-d**. In these particular derivatives, compound **12a** without any substitution on aryl ring showed moderate activity against both the tested cell lines as compared to that of standard drug. Compound **12b** with chloro substituent on aryl hydrazide part showed very good activity with IC_{50} values $0.858 \pm 0.0049 \mu\text{M}$, however activity against MCF-7 cell line remained moderate. On replacing chloro with nitro group in compound **12c** resulted in drop of activity against A549 cell line, while activity against MCF-7 cell line almost remained same. Compound **12d** with pyridine ring exhibited poor activity against A549 cell line but there was improvement in activity against MCF-7 cell line.

Compounds **14b** with chloro and **14c** with dichloro substituents, showed very good activity against A549 cell line with IC_{50} values 1.822 ± 0.029 and $1.86 \pm 0.023 \mu\text{M}$ respectively as compared to compound **14a** without any substituent on aryl hydrazine. Against MCF-7 cell line, only compound **14b** showed good activity with IC_{50} value $4.19 \pm 1.27 \mu\text{M}$ compared to standard drug. Out of all the screened compounds, compound **12b** with IC_{50} values $0.858 \pm 0.0049 \mu\text{M}$ against A549 cell line and compound **10d** with IC_{50} values $2.07 \pm 0.065 \mu\text{M}$ against MCF-7 cell line were selected for further study for LDH assay, Trypan blue assay and ROS activity.

2.2.4 LDH assay:

There are many mechanisms by which an anticancer compound exerts its effect on cancer cells *in vitro*. Apoptosis and necrosis are the most acknowledged mechanisms. To understand the mode of cytotoxicity of compounds **12b** and **10d** in A549 and MCF-7 cancer cell lines LDH Assay was performed (**Fig-2.17**).

At lower concentration of both compounds (IC_{50}), the LDH release was very low which revealed that at this concentration the prevalent mechanism of cytotoxicity was apoptosis. At increased concentration of compounds, the LDH release increases significantly, at higher concentration treated cells changed its fate toward the necrosis from apoptosis. However, the preferred mechanism of cytotoxicity for compounds **12b** and **10d** is apoptosis at IC_{50} concentration.

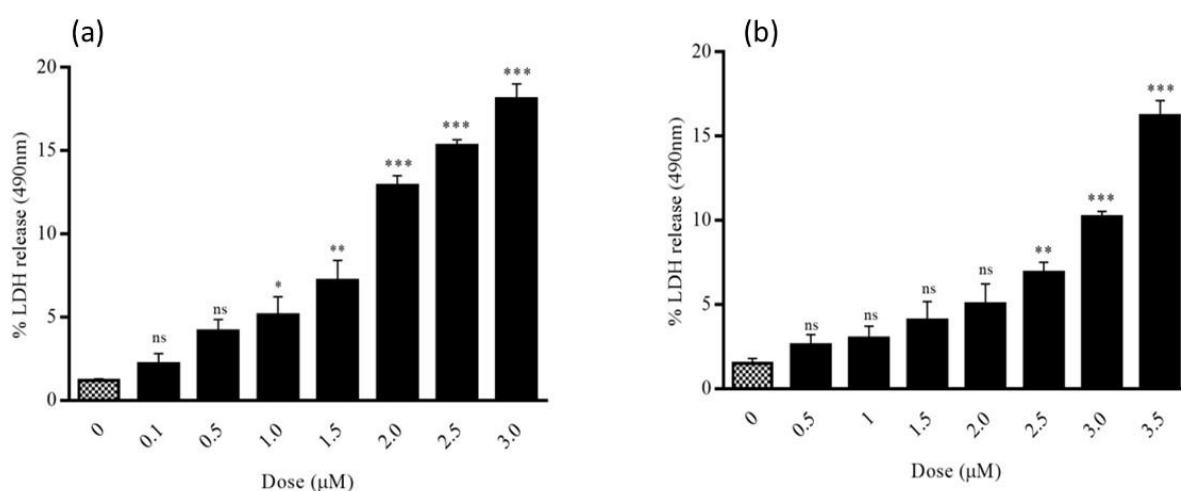


Figure- 2.17 In LDH assay (a) and (b): Representation of cytosolic enzyme LDH (a) activity of LDH in A549 cell line (b) activity of LDH in MCF- 7 cell line. Cells were treated with 0.1, 0.5, 1.0, 1.5, 2.0, 2.5, 3.0 μM concentrations of compound **12b** and 0.1, 0.5, 1.0, 1.5, 2.0, 2.5, 3.0, 3.5 μM concentrations of compound **10d**. (***) $p \leq .001$, (**) $p < .01$, (*) $p < .05$)

2.2.5 Ethidium bromide/acridine orange staining assay:

For A549 cell line and MCF-7 cell line, further experimental confirmation is required to explain the effect of compound **12b** and compound **10d** on cancer cell lines respectively. In order to reaffirm the findings of LDH assay, the EtBr/AO staining assay was performed with compound **12b** and compound **10d**.

Acridine orange is a vital dye that stains both live and dead cells however, ethidium bromide stains only the cells that have lost their membrane integrity. EtBr/AO dye stains, necrotic cells red, live cells green, early apoptotic cell's nuclei green but with visible condensation whereas, late apoptotic cell's nuclei orange with condensation and fragmentation. Cells were treated with IC₅₀ concentration of compound **10d** and compound **12b**, it was found that most of the cells of A549 cell line (**Fig-2.18 a-c**) were under late apoptosis, there were no cells under necrosis whereas, in MCF-7 cell line (**Fig-2.18 d-f**) most of the cells were under early apoptosis with few under necrosis. Number of the cells under apoptosis and necrosis were negligible in control cell lines. Which confirmed the LDH assay finding that compound **10d** and compound **12b** exhibits cytotoxic activity in both cell lines via apoptosis.

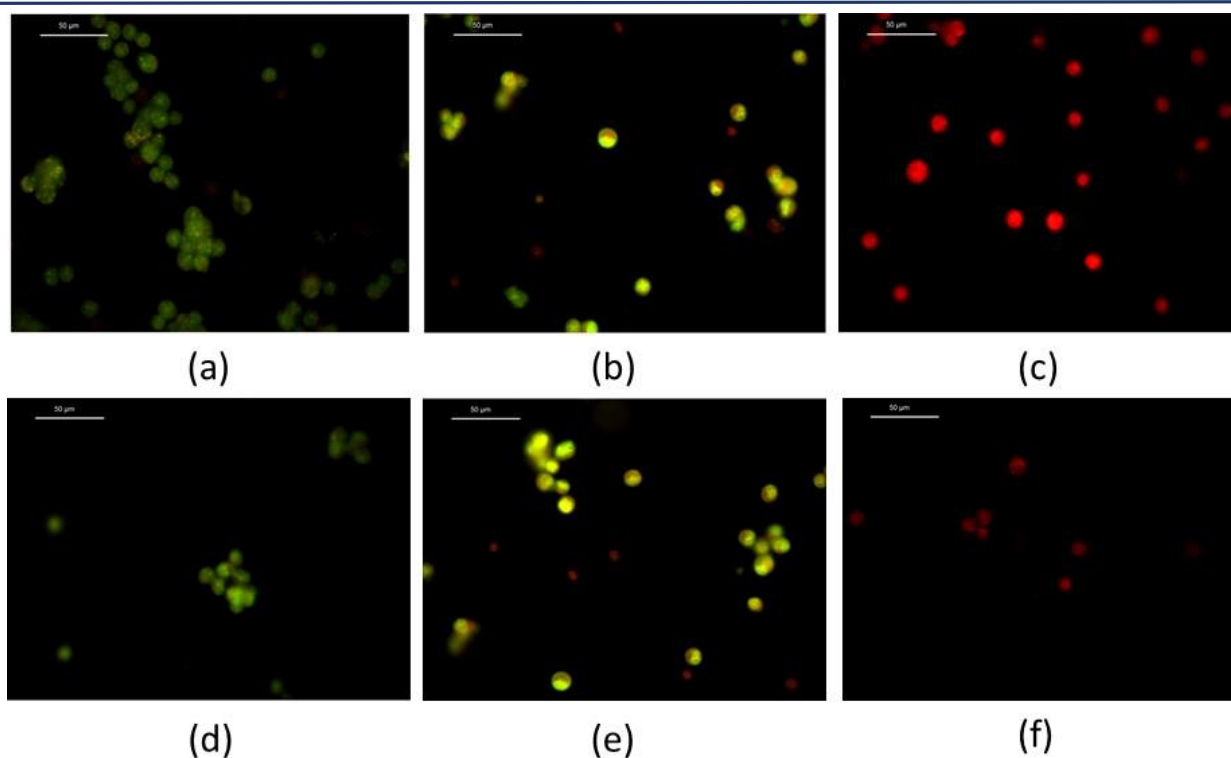


Figure- 2.18 EtBr/AO assay: EtBr/AO assay was performed with A549 cell line (a,b,c) for compound **12b** and MCF-7 (d,e,f) for compound **10d**. (a,b,c). For compound **12b**, (a-c) images represent control, IC₅₀ conc. of compound **12b** treated and positive control in A549 cell line. Images (d,e,f) represent control, IC₅₀ conc. of compound **10d** treated and positive control in MCF-7 cell line respectively

2.2.6 Trypan blue:

To confirm, that loss of percentage viability was either due to cell death or due to cell proliferation inhibition effect of compound **10d** and **12b**, Trypan blue assay was performed in both A549 and MCF-7 cell lines. The percentage cell death at IC₅₀ concentration for compound **10d** is $45\% \pm 2.68\%$ in MCF- 7 cell line and for compound **12b** it was approx. $36\% \pm 3\%$ in A549 cell line and (**Fig-2.19**), from this it can be construed that compound **10d** is cytotoxic towards the MCF-7 whereas it might be cytotoxic or cytostatic toward A549 cell line, while compound **12b** is cytotoxic towards A549 cell line and it might be cytostatic or cytotoxic towards MCF-7 cell line.

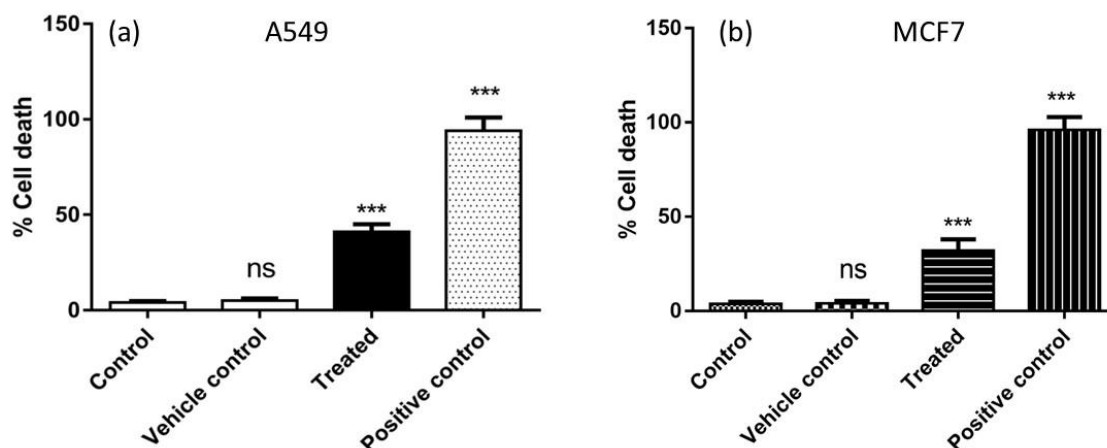


Figure- 2.19 Trypan blue assay: Percentage cell death of A549 and MCF-7 cell line DMF treated, compound treated (IC_{50} conc. **12b** and **10d**) and positive control. (***) $p \leq .001$, ** $p < .01$, * $p < .05$)

2.2.7 DCFH-DA Assay:

Most of the chemotherapeutics, elevates ROS (Reactive Oxygen Species) beyond the threshold limit to exert cytotoxicity to cancer cell [14]. The elevated ROS play a vital role in induction of apoptosis via caspase 8 dependent and Fas-associated cell death [15] as well via p53 dependent pathway. Ramsey and Sharpless [16] reported that P⁵³ is a redox-sensitive transcription factor that senses the increased ROS and initiates the apoptotic death in cancer cells. Hence, herein, we investigated the ROS concentration in compound **12b** and **10d** in A549 and MCF-7 cell line respectively. The result vividly confirmed the increased ROS level in both cell lines at IC_{50} concentration. (**Fig-2.20**)

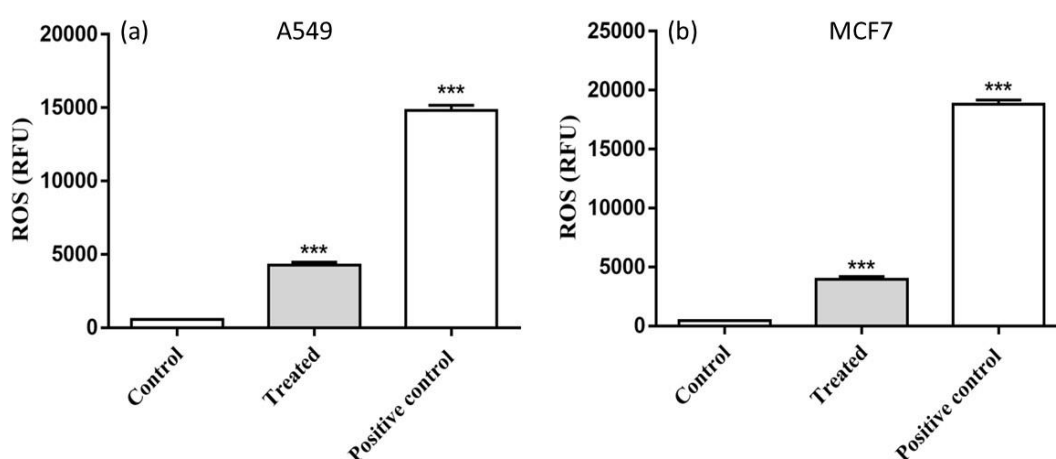


Figure- 2.20 Estimation of intracellular reactive oxygen species level by using DCFH-DA for compound **12b** in A549 fig (a) and **10d** in MCF-7 fig (b) respectively. (***) $p \leq .001$)

2.2.8 *In-silico* based ADME and Toxicity study:

The drug-likeness of compounds were predicted using SwissADME (Table-2.2). To be a drug-like candidate, the compounds should follow Lipinski's Rule of Five ($\text{clogP} \leq 5$, molecular weight ≤ 500 , the number of hydrogen bond acceptors ≤ 10 and donor ≤ 5) which predict lipophilicity, critical molecular weight and chemical structure, and probability of crossing the blood-brain barrier (BBB). The compound violating more than one of these rules will be poor in terms of bioavailability and not be orally active, hence, cannot be used as drug without modification [17]. The compound **12b** was satisfying all four criteria of good drug candidate *viz.*, Molecular weight 386.83g/mol; octanol/water partition coefficient *viz.*, 4.03 ($\log P_{o/w}$ less than 5), the number of hydrogen donor *viz.*, 2 and the number of hydrogen acceptor *viz.*, 4. In addition, GI absorption, Blood brain barrier permeability is also predicted which are again under acceptable limit (GI absorption is high, BBB permeability not present and moderately soluble). Similarly, the **10d** was analysed and showed M.W. of 521.42g/mol, slightly higher than the accepted limit with no H donor group, 6 -H acceptor group and with $\log P_{o/w}$ 3.98. The allowed violation of rule of five is one, hence the compound was still a good drug candidate for further study. The compound also showed a high GI absorption as well as negligible BBB permeability however moderate solubility require further consideration. The toxicity of compounds was predicted using ProTox-II webserver developed by Drwal *et al.*, [18] the parameters such as rat oral acute toxicity with special reference to median lethal dose (LD_{50}) as mg/kg, organ toxicity especially hepatotoxicity, immunotoxicity, genetic toxicity endpoints especially cytotoxicity, mutagenicity and carcinogenicity, were predicted for both the compounds. The LD_{50} for compound **10d** and **12b** was 1000mg/kg hence, classified to class IV ($300 \leq LD_{50} \leq 2000$). According to GHS class I is the most toxic and class VI is non-toxic. [18] However, the IC_{50} concentration of compounds was found to be very less than LD_{50} hence, it will not pose any toxicity if given orally. The derivative **12b** was showing moderate hepatotoxicity, however, carcinogenicity, immunotoxicity and mutagenicity was not observed. In the compound **10d** there were no Hepatotoxicity, no carcinogenicity, no immunotoxicity and no mutagenicity was observed. Hence, both the compounds can be taken further as anticancer drug candidate for detail analysis.

Table 2.2: ADMET properties of compounds 12b and 10d

ADMET properties	12b	10d
M.W (g/mol)	386.83	521.42
No of H-donor group	2	0
No of H-acceptor	4	6
logP _{o/w}	4.03	3.98
GI absorption	High	High
BBB permeability	No	No
Log S	Moderately soluble	Moderately soluble
LD50	1000mg/kg	1000mg/kg
Hepatotoxicity (dilli)	Moderate active	Inactive
Carcinogenicity	Inactive	Inactive
Immunotoxicity	Inactive	Inactive
Mutagenicity	Inactive	Inactive

2.3 DFT calculation:

DFT calculations were carried out to explore conformational behavior of the two most active compounds **10d** and **12b**. The ground state geometries of these compounds were optimized by applying the B3LYP method 6-31G(d) basis set in gas phase. Initially compounds **10d** and **12b** were optimized by applying the B3LYP method and 6-31F(d) basis set in gas phase. Ground state geometries of compounds **10d** and **12b** were optimized. (Fig-2.21) The predicted plot of frontier molecular orbitals (FMOs) HOMO (highest occupied) and LUMO (lowest unoccupied) molecular orbitals are as shown in Fig-2.21.

For benzofuran carboxamide containing piperazine moiety **10d**, the LUMO shows electron density on phenyl ring attached to piperazine sulphonamide, while in HOMO of **10d** it is observed that the electron density is shifted on benzofuran ring from piperazine sulphonamide ring contributing negligible by propyl chain. In compound **12b** LUMO shows the electron density is distributed on the whole molecule that is benzofuran as well as phenyl hydrazide ring (Fig-2.21) contributing negligible to propyl chain. while in compound **12b** the HOMO shows shifting electron density from phenyl ring of hydrazide to the benzofuran carboxamide. For compound **12b** the highest occupied molecular orbitals (HOMO) are localized on benzofuran carboxamide core. Fig- 2.21(b) shows molecular electrostatic potential maps (MEP) of compounds **10d** and **12b**, thus support the highest activity of these two compounds.

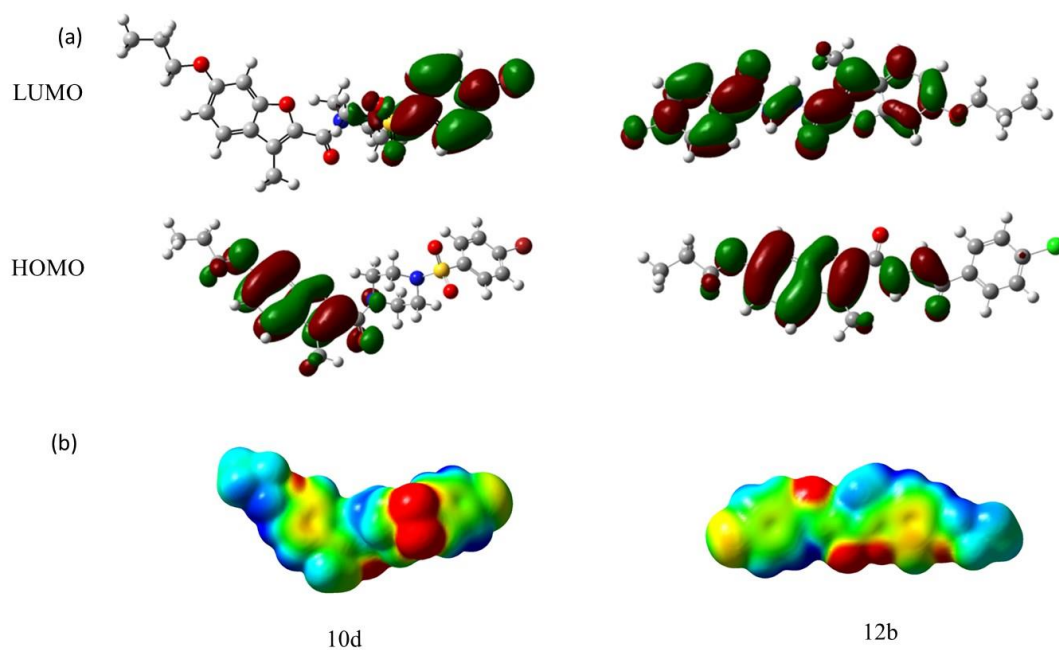


Figure- 2.21 DFT calculation data for compound **10d** and **12b** (a) frontiers molecular orbitals (HOMO and LUMO) diagram obtained from calculation at B3LYP/6-31G (d, p) level, (b) shows the molecular electrostatic potential maps (MEP) of compounds **10d** and **12b**

2.4 Conclusion

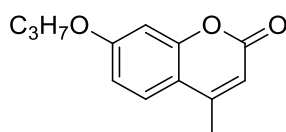
In conclusion, a series of substituted amide derivatives of benzofuran carboxylic acid were synthesized and evaluated for their anticancer activity against A549 and MCF-7 cell lines. Based on MTT assay, compound **10d** has shown very good selectivity for MCF-7 breast cancer cell line and compound **12b** showed excellent activity against A549 lungs cancer cell line. The cytotoxic studies of compound **12b** and **10d** have shown the apoptosis in both A549 and MCF-7 cell lines using LDH assay, Trypan blue assay and the EtBr/AO assay. The increased level of ROS concentration in compound **12b** and **10d** in A549 and MCF-7 cell line at IC₅₀ value confirmed apoptosis. The *In-silico* based ADME and toxicity study of compounds **12b** and **10d** indicated that both compounds showed drug-likeness and can be studied further in detail as anticancer drug.

2.5 Experimental

2.5.1 General Chemistry

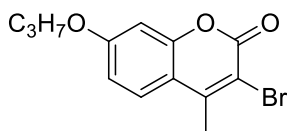
Reagent grade chemicals and solvents were purchased from commercial supplier and used after purification. TLC was performed on silica gel F254 plates (Merck). For column chromatographic purification Acme's silica gel (60-120 mesh) was used. Melting points were measured in open capillary tubes, using a Rolex melting point apparatus. IR spectra were recorded as KBr pellets on Perkin Elmer RX 1 spectrometer. ^1H NMR and ^{13}C NMR spectral data were recorded on Advance Bruker 400 spectrometer (400 MHz) with CDCl_3 or DMSO-d_6 as solvent and TMS as internal standard. J values are in Hz. Mass spectra were determined by ESI-MS, using a Shimadzu LCMS 2020 apparatus. Elemental analyses were recorded on Thermosinnigan Flash 11-12 series EA. 4-methyl-7-propoxy-2H-chromen-2-one, 3-bromo-4-methyl-7-propoxy-2H-chromen-2-one, 3-methyl-6-propoxybenzofuran-2-carboxylic acid and substituted phenyl piperazine and substituted benzofuran carboxamide derivatives were prepared according to literature method [2,19,20,21].

Preparation of 4-Methyl-7-propoxy-2H-chromen-2-one (6)



A mixture of compound 7-hydroxy 4 methyl coumarin (45.71mmol, 1.0 eq) and anhydrous potassium carbonate (68.56 mmol, 1.5 eq) in N, N-dimethyl formamide (DMF) (50.0 mL) was stirred for 10 hours at rt. To this mixture, alkyl bromide (50.28 mmol, 1.1 eq) was added and resulting mixture was stirred at rt for 12 h. The completion of reaction was checked by TLC. After completion of reaction, reaction mixture was poured into crushed ice. The solid separated out was filtered, washed with cold water and recrystallized from ethanol to give compounds **6** with 90% yield.

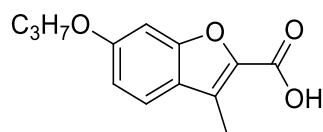
Preparation of 3-Bromo-4-methyl-7-propoxy-2H-chromen-2-one (7)



To a clear solution of compound **6** (32.11mmol, 1.0eq) in glacial acetic acid (100 ml) was added drop wise a solution of bromine in acetic acid (1.65 ml, 32.11mmol, 1.0 eq) using dropping funnel. The reaction mixture was stirred at room temperature for 16 hours. The completion of reaction was checked by TLC. After completion of reaction, reaction mixture was poured into ice water. The solid separated out was filtered, washed with cold water and

dried. The crude product recrystallized from ethanol to give pale yellow solid compounds **7** with yield 82%.

Preparation of 3-Methyl-6-propoxybenzofuran-2-carboxylic acid (8)



A solution of compound **7** (23.64 mmol, 10eq) in 10%ethanolic KOH (100ml) was reflux for 3h in an oil bath. The completion reaction was checked by TLC. After completion of reaction excess of ethanol distilled under reduced pressure and reaction mixture was poured into crushed ice. The solution was acidified to P^H 2 to give solid. The solid separated out was filtered, washed with cold water, dissolved in saturated solution of NaHCO₃ and re-filtered to remove insoluble impurity. The filtrate was acidified using conc. HCl to P^H 2 to give solid. Solid separated out was filtered, washed with cold water and dried. The crude product was recrystallized from ethanol to give light brown solid compound **8**.

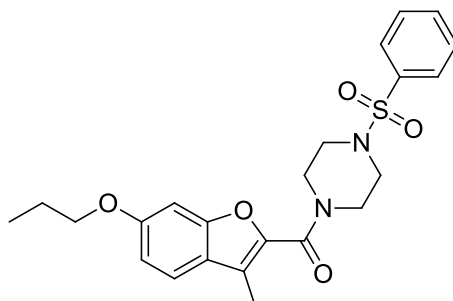
White Solid; Yield: 88 %; M.P: 124-126 °C; IR (KBr) 2970, 2928, 2865, 1888, 1632, 1608, 1494, 1450, 1431, 1387, 1347, 1327, 1297, 1276, 1236, 1214, 1166, 1113, 1097, 1067, 1048, 1001, 982, 961, 934, 890, 854, 821, 759, 744 cm⁻¹; ¹H-NMR (400 MHz, CDCl₃): δ 1.07 (t, *J* = 7.2Hz, 3H), 1.81-1.90 (m, 2H), 2.41 (s, 3H), 3.13 (br s, 4H), 3.89 (br s, 4H), 3.97 (t, *J* = 6.4Hz, 2H), 6.91-6.95 (m, 2H), 7.43 (d, *J* = 9.2Hz, 1H), 7.56-7.60 (m, 2H), 7.64-7.68 (m, 1H), 7.77-7.79 (m, 2H).

General Procedure for preparation of compounds 10a-e/12a-d/14a-c:

compound **8** (0.90mmol, 1eq), EDC (1.35 mmol, 1.5eq) and HOBt (1.8 mmol, 1 eq) in DCM (15ml) were stirred at room temperature for 10 min then added Substituted phenyl piperazine sulphonamide **9**/ substituted hydrazides **11**/ aryl hydrazines **13** in the mixture of compound **8** and TEA (1.8 mmol, 2eq) added to the same reaction mixture at 0-5°C. The resultant mixture was bringing to room temperature and stirred for 6hr. After the reaction completion, consumption of both the starting materials were confirmed by TLC. Reaction mixture was washed with water and NaHCO₃ solution (3×40 mL), dried over anhydrous Na₂SO₄ and DCM evaporated in vacuum.

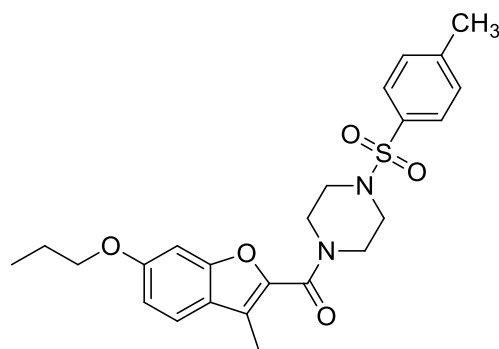
Characterization data for compounds 10a-e, 12a-d and 14a-c:

(3-Methyl-6-propoxybenzofuran-2-yl) (4-(phenylsulfonyl) piperazin-1-yl) methanone (10a)



White Solid; Yield: 88 %; M.P: 124-126 °C; IR (KBr) 2970, 2928, 2865, 1888, 1632, 1608, 1494, 1450, 1431, 1387, 1347, 1327, 1297, 1276, 1236, 1214, 1166, 1113, 1097, 1067, 1048, 1001, 982, 961, 934, 890, 854, 821, 759, 744 cm^{-1} ; $^1\text{H-NMR}$ (400 MHz, CDCl_3): δ 1.07 (t, $J = 7.2\text{Hz}$, 3H), 1.81-1.90 (m, 2H), 2.41 (s, 3H), 3.13 (br s, 4H), 3.89 (br s, 4H), 3.97 (t, $J = 6.4\text{Hz}$, 2H), 6.91-6.95 (m, 2H), 7.43 (d, $J = 9.2\text{Hz}$, 1H), 7.56-7.60 (m, 2H), 7.64-7.68 (m, 1H), 7.77-7.79 (m, 2H); $^{13}\text{C-NMR}$ (100 MHz, CDCl_3): δ ppm 9.26, 10.55, 22.50, 45.44, 46.27, 70.06, 96.06, 113.33, 120.88, 122.13, 125.32, 129.31, 133.25, 135.35, 154.56, 159.56, 160.95; Anal. calc. for $\text{C}_{23}\text{H}_{26}\text{N}_2\text{O}_5\text{S}$ C, 62.42; H, 5.92; N, 6.33; S, 7.25; found: C, 62.35; H, 5.77; N, 6.23; S, 7.15; ESI-MS: 442.95 $[\text{M}^+]$.

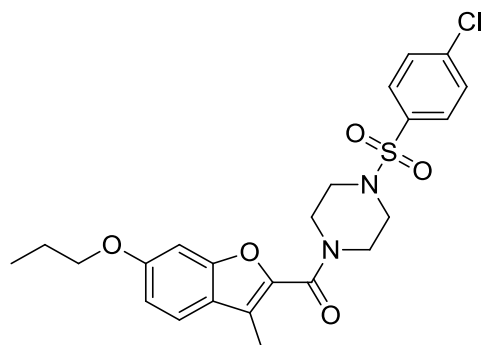
(3-Methyl-6-propoxybenzofuran-2-yl) (4-tosylpiperazin-1-yl) methanone (10b)



White Solid, Yield: 90%; M.P: 130-132°C; IR (KBr) 2970, 2927, 2870, 1638, 1608, 1493, 1452, 1387, 1346, 1297, 1160, 1096, 1048, 982, 890, 820, 760, 727 cm^{-1} ; $^1\text{H-NMR}$ (400 MHz, CDCl_3): δ 1.07 (t, $J = 7.2\text{Hz}$, 3H), 1.82-1.90 (m, 2H), 2.41 (s, 3H), 2.47 (s, 3H), 3.10 (br s, 4H), 3.88 (br s, 4H), 3.97 (t, $J = 6.4\text{Hz}$, 2H), 6.92-6.94 (m, 2H), 7.37 (d, $J = 8.0\text{ Hz}$, 2H), 7.44 (d, $J = 9.2\text{ Hz}$, 1H), 7.67 (d, $J = 8.0\text{ Hz}$, 2H); $^{13}\text{C-NMR}$ (100 MHz, CDCl_3): δ ppm 9.26, 10.56, 21.59, 22.51, 45.45, 46.28, 70.06, 96.08, 113.30, 120.86, 122.15, 123.62, 127.69, 129.91,

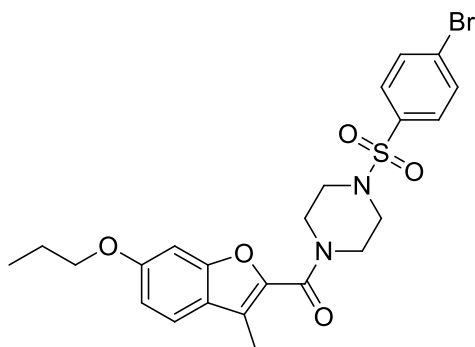
132.25, 142.22, 144.15, 154.54, 159.53, 160.89; Anal. calc. for $C_{24}H_{28}N_2O_5S$ C,63.14; H,6.18; N,6.14; S,7.02; found: C,63.09; H,6.11; N,6.09; S,6.93; ESI-MS: 457.10[M+H]⁺.

(4-((4-Chlorophenyl)sulfonyl)piperazin-1-yl)(3-methylbenzofuran-2-yl)methanone (10c)



White Solid; Yield=86%; M.P.:140-142°C; IR (KBr) 2967, 2926, 2872, 1622, 1588, 1494, 1432, 1391, 1348, 1295, 1275, 1238, 1165, 1121, 1097, 1010, 982, 946, 888, 824, 765, 718 cm^{-1} ; ¹H-NMR (400MHz,CDCl₃): δ 1.06 (t, *J* = 7.2Hz, 3H), 1.82-1.88 (m, 2H), 2.42 (s, 3H), 3.13 (br s, 4H), 3.89(br s, 4H), 3.97 (t, *J* = 6.4Hz, 2H), 6.92-6.95 (m, 2H), 7.42-7.44(m,1H), 7.53-7.56 (m, 2H), 7.68-7.73 (m, 2H); ¹³C-NMR (100 MHz, CDCl₃): δ ppm 9.28, 10.55, 22.51, 46.21, 70.06, 96.06, 113.34, 120.90, 122.14, 122.14, 123.90, 129.12, 129.65, 133.90, 139.88, 142.12, 154.54, 159.58, 160.89;Anal.calc.for $C_{23}H_{25}ClN_2O_5S$ C,57.92; H,5.28; N,5.87; S,6.72; found: C,57.87; H,5.18; N,5.75; S,6.63; ESI-MS: 477.00 [M+H]⁺.

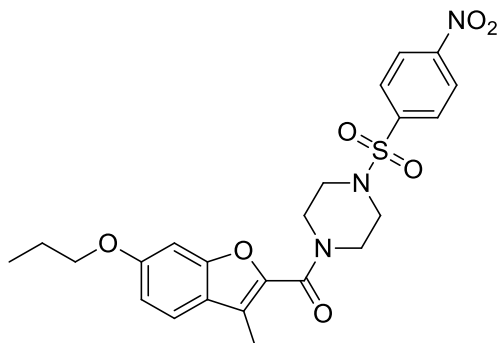
(4-((4-Bromophenyl) sulfonyl) piperazin-1-yl) (3-methylbenzofuran-2-yl)methanone (10d)



Yield-90%; M.P.-154-156°C; IR (KBr) 2965, 2926, 2871, 1621, 1593, 1574, 1493, 1468, 1443, 1430, 1387, 1347, 1295, 1274, 1238, 1163, 1121, 1098, 1066, 1008, 981, 946, 885, 820, 758, 712 cm^{-1} ; ¹H-NMR (400 MHz, CDCl₃): δ 1.06 (t, *J* = 7.6 Hz, 3H), 1.83-1.88 (m, 2H), 2.41 (s, 3H), 3.12 (br s, 4H), 3.88(br s, 4H), 3.96 (t, *J* = 6.4Hz, 2H), 3.97 (t, *J* = 6.4Hz, 2H), 6.91-6.94 (m, 2H), 7.42-7.44 (q, 1H), 7.62(t, *J* = 6.8Hz, 2H), 7.71(d, *J* = 8.4Hz, 2H); ¹³C-NMR (100 MHz, CDCl₃): δ ppm 9.29, 10.56, 22.51, 70.06, 96.06, 113.35, 120.90, 122.14, 123.92, 128.41, 129.20, 132.63, 134.43, 142.12, 154.54, 159.58, 160.89; Anal.calc.for $C_{23}H_{25}BrN_2O_5S$

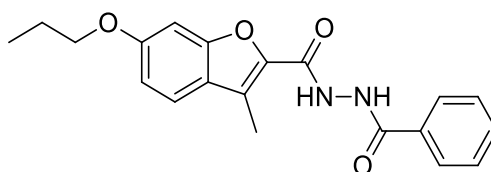
C,52.98; H,4.83; N,5.37; S,6.15; found: C,52.83; H,4.76; N,5.297; S,6.10; ESI-MS: 522.00 [M+H]⁺.

(3-Methyl-6-propoxybenzofuran-2-yl)(4-((4-nitrophenyl)sulfonyl)piperazin-1-yl)methanone (10e)

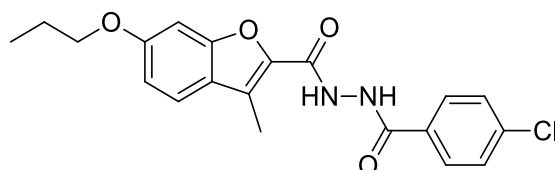


White solid, Yield: 85 %; M.P: 188-190°C; IR (KBr) 3111, 3069, 2968, 2927, 2872, 1622, 1575, 1543, 1494, 1431, 1402, 1351, 1312, 1295, 1275, 1238, 1163, 1122, 1098, 1065, 1010, 982, 949, 886, 856, 821, 812, 788, 758, 741 cm⁻¹; ¹H-NMR(400 MHz, CDCl₃): ¹H-NMR (400 MHz, CDCl₃): δ 1.08 (t, *J* = 7.4Hz, 3H), 1.84-1.90 (m, 2H), 2.42 (s, 3H), 3.20 (br s, 4H), 3.92 (br s, 4H), 3.97 (t, *J* = 6.4Hz, 2H), 6.91-6.95 (m, 2H), 7.44 (d, *J* = 8.4Hz, 1H), 7.99 (d, *J* = 7.0Hz, 2H), 8.43(d, *J* = 7.0Hz, 2H); ¹³C-NMR (100 MHz, CDCl₃): δ ppm 9.30, 10.56, 22.51, 46.19, 70.08, 76.74, 77.06, 96.03, 113.39, 120.86, 122.11, 124.23, 124.58, 128.91, 141.54, 141.99, 142.00, 150.39, 154.54, 159.67, 160.88; Anal. calc. for C₂₃H₂₅N₃O₇S; C,56.66; H,5.17; N,8.62; S,6.58; found: C,56.59; H,5.12; N,8.60; S,6.53; ESI-MS: 487.70 [M⁺].

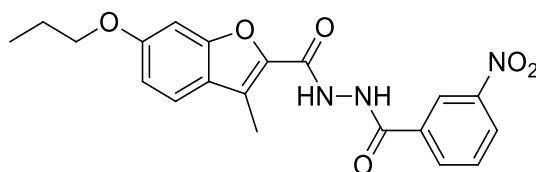
***N'*-Benzoyl-3-methyl-6-propoxybenzofuran-2-carbohydrazide (12a)**



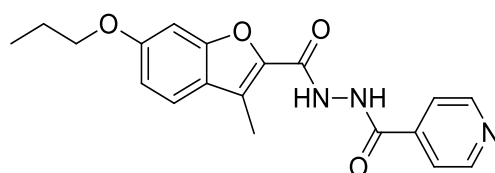
White Solid; Yield: 86%; M.P:160-162°C; IR (KBr) 3213, 2966, 2309, 1632, 1604, 1514, 1491, 1381, 1268, 1247, 1166, 1146, 1125, 1096, 1075, 981, 818, 771 cm⁻¹; ¹H-NMR (400 MHz, DMSO-*d*₆): δ 1.02 (t, *J* = 7.4Hz,3H), 1.76-1.82 (m, 2H), 2.53 (s, 3H), 4.04 (t, *J* = 6.8Hz, 2H), 7.00(dd, *J* = 8.4Hz, 2.0Hz, 2H), 7.15 (d, *J* = 2.0Hz, 1H), 7.53-7.57 (m,2H), 7.61-7.67 (m, 2H), 7.93-7.95 (m, 2H), 10.47 (br s, 2H); ¹³C-NMR (100 MHz, DMSO-*d*₆): δ ppm 9.24, 10.91, 22.45, 70.03, 96.62, 113.67, 122.06, 122.49, 123.30, 127.96, 129.00, 132.38, 132.97, 141.63, 154.70, 159.48, 159.90, 166.28; Anal. calc. for C₂₀H₂₀N₂O₄; C,68.17; H,5.72; N,7.95; found: C,68.09; H,5.57; N,7.89; ESI-MS: 353.00 [M+H]⁺.

***N'*-(4-Chlorobenzoyl)-3-methyl-6-propoxybenzofuran-2-carbohydrazide (12b)**

White solid; Yield: 92 %; M.P: 162-164°C; IR (KBr) 3205, 3055, 3004, 2965, 2878, 1676, 1633, 1601, 1514, 1434, 1382, 1346, 1308, 1247, 1165, 1146, 1098, 1071, 980, 913, 880, 844, 751 cm^{-1} ; $^1\text{H-NMR}$ (400 MHz, $\text{DMSO-}d_6$): δ 1.09 (t, $J = 7.2\text{Hz}$ 3H), 1.86-1.91 (m, 2H), 2.60 (s, 3H), 3.98(t, $J = 6.4\text{Hz}$, 2H), 6.96 (d, $J = 7.2\text{Hz}$, 2H), 7.44 (m, 3H), 7.85 (d, $J = 8.0\text{Hz}$, 2H), 9.34 (s, 1H), 9.52 (s, 1H); $^{13}\text{C-NMR}$ (100 MHz, $\text{DMSO-}d_6$): δ ppm 9.25, 10.93, 22.5, 70.04, 96.62, 113.7, 122.1, 122.5, 123.41, 129.2, 129.90, 131.72, 137.23, 141.6, 154.71, 159.44, 159.94, 165.25; Anal. calc. for $\text{C}_{20}\text{H}_{19}\text{ClN}_2\text{O}_4$; C,62.10; H,4.95; N,7.24; found: C,61.97; H,4.87; N,7.16; ESI-MS: 386.60[M⁺].

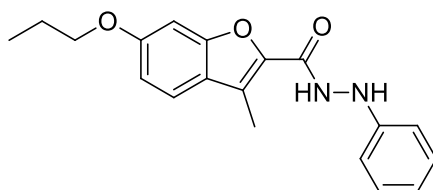
***3-Methyl-N'*-(3-nitrobenzoyl)-6-propoxybenzofuran-2-carbohydrazide (12c)**

White Solid; Yield: 90%; M.P: 182-184°C; IR (KBr) ; 3205, 2969, 2877, 1631, 1532, 1473, 1433, 1349, 1298, 1265, 1148, 1074, 812, 716 cm^{-1} ; $^1\text{H-NMR}$ (400 MHz, $\text{DMSO-}d_6$): δ 1.02 (t, $J = 7.2\text{ Hz}$, 3H), 1.74-1.82 (m, 2H), 2.53 (s, 3H), 4.04 (t, $J = 6.4\text{Hz}$, 2H), 7.00 (dd, $J = 8.8\text{Hz}$, 2.0Hz, 1H), 7.15 (d, $J = 1.6\text{Hz}$, 1H), 7.65 (d, $J = 8.8\text{Hz}$, 1H), 7.84-7.88 (m, 1H), 8.39 (d, $J = 7.8\text{Hz}$, 1H), 8.45(dd, $J = 8.2\text{Hz}$, 1.6Hz, 1H), 8.77(s, 1H), 10.65(br s, 1H); $^{13}\text{C-NMR}$ (100 MHz, $\text{DMSO-}d_6$): δ ppm 9.24, 10.91, 22.46, 70.06, 96.62, 113.64, 122.01, 122.52, 122.63, 123.30, 130.84, 134.26, 141.64, 148.26, 154.69, 158.94, 159.90, 164.08; Anal. calc. for $\text{C}_{20}\text{H}_{19}\text{N}_3\text{O}_6$ C,60.45; H,4.82; N,10.57; found: C,60.38; H,4.79; N,10.50; ESI-MS: 397.90[M⁺].

***N'*-(3-Methyl-6-propoxybenzofuran-2-carbonyl)isonicotinohydrazide (12d)**

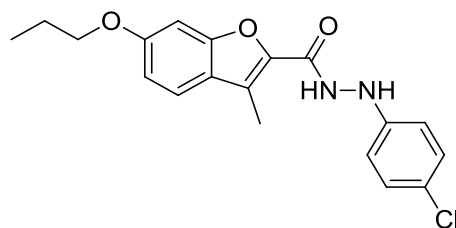
White solid, Yield: 78%; M.P: 166-168 °C; IR (KBr) 3255, 3055, 2967, 2937, 2877, 1724, 1667, 1600, 1551, 1499, 1460, 1196, 1128, 1018, 983, 960, 843, 770 cm^{-1} ; $^1\text{H-NMR}$ (400 MHz, $\text{DMSO-}d_6$): δ 1.07 (t, 3H), 1.84-1.90 (q, 2H), 2.56 (s, 3H), 3.97 (t, 2H), 6.94-6.97 (m, 2H), 7.47 (s, 1H), 7.73 (d, $J = 8.4\text{Hz}$, 2H), 8.76 (s, 2H); $^{13}\text{C-NMR}$ (100 MHz, $\text{DMSO-}d_6$): 9.25, 10.93, 22.46, 70.05, 96.63, 113.72, 121.82, 122.12, 122.47, 123.59, 139.97, 141.46, 150.98, 154.73, 159.30, 159.98, 164.74; Anal. calc. for $\text{C}_{19}\text{H}_{19}\text{N}_3\text{O}_4$; C,65.78; H,6.57; N,10.96; found: C,65.80; H,6.55; N,10.91; ESI-MS: 354.05 $[\text{M}+\text{H}]^+$.

3-Methyl-*N'*-phenyl-6-propoxybenzofuran-2-carbohydrazide (14a)



White solid; Yield: 90%; M.P: 120-122°C; IR (KBr) 3222, 2967, 2932, 2875, 2854, 1655, 1603, 1494, 1469, 1432, 1391, 1379, 1356, 1345, 1317, 1282, 1271, 1235, 1161, 1133, 1121, 1083, 1070, 1059, 980, 945, 908, 884, 825, 816, 751, 692, 636 cm^{-1} ; $^1\text{H-NMR}$ (400 MHz, CDCl_3): δ 1.11 (t, $J = 7.4\text{Hz}$, 3H), 1.85-1.94 (m, 2H), 2.60 (s, 3H), 4.01 (t, $J = 6.4\text{Hz}$, 2H), 6.29 (d, $J = 4.0\text{Hz}$, 1H), 6.93-7.00 (m, 1H), 7.26-7.30 (m, 2H), 7.51 (d, $J = 8.8\text{Hz}$, 1H), 8.27 (s, 1H); $^{13}\text{C-NMR}$ (100 MHz, CDCl_3): δ ppm 9.01, 10.58, 22.52, 70.10, 96.10, 113.47, 113.74, 121.33, 121.42, 122.60, 124.84, 129.28, 140.62, 148.17, 154.84, 160.13, 160.44; Anal. calc. for $\text{C}_{19}\text{H}_{20}\text{N}_2\text{O}_3$; C,70.35; H,6.21; N,8.64; found: C,70.24; H,6.13; N,8.58; ESI-MS: 324.90 $[\text{M}]^+$.

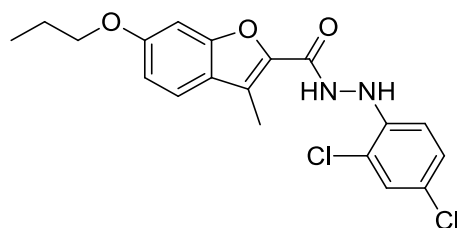
***N'*-(4-Chlorophenyl)-3-methyl-6-propoxybenzofuran-2-carbohydrazide (14b)**



White Solid; Yield: 89%; M.P: 140-142°C; IR (KBr): 3360, 3231, 3058, 2961, 2939, 2917, 2873, 1673, 1653, 1611, 1535, 1491, 1468, 1434, 1395, 1380, 1347, 1302, 1291, 1269, 1228, 1165, 1128, 1090, 1076, 1045, 1017, 1004, 983, 951, 902, 857, 820, 790, 764, 743 cm^{-1} ; $^1\text{H-NMR}$ (400 MHz, CDCl_3): δ 1.09 (t, $J = 7.6\text{Hz}$, 3H), 1.84-1.93 (m, 2H), 2.60 (s, 3H), 4.01 (t, $J = 6.4\text{Hz}$, 2H), 6.91 (d, $J = 3.2\text{Hz}$, 2H), 6.96-6.99 (m, 2H), 7.21 (d, $J = 8.8\text{ Hz}$, 2H), 7.50 (d, $J = 9.2\text{Hz}$, 1H), 8.28 (s, 1H); $^{13}\text{C-NMR}$ (100 MHz, CDCl_3): δ ppm 9.01, 10.55, 22.50, 70.10, 96.08, 113.56, 114.93, 121.36, 122.51, 125.27, 126.08, 129.15, 140.35, 146.79, 154.90,

160.26, 160.63; Anal. calc. for C₁₉H₁₉ClN₂O₃; C,63.60; H,5.34; N,7.81; found: C,63.58; H,5.31; N,7.76; ESI-MS: 358.90 [M⁺].

***N'*-(2,4-Dichlorophenyl)-3-methyl-6-propoxybenzofuran-2-carbohydrazide (14c)**



Pale Yellow Solid; Yield: 92%; M.P: 136-138°C; IR (KBr): 3102, 3039, 3009, 2964, 2934, 2910, 2878, 1653, 1621, 1600, 1541, 1493, 1474, 1432, 1386, 1355, 1312, 1299, 1270, 1231, 1161, 1120, 1099, 1077, 1047, 1013, 982, 954, 902, 890, 855, 820, 810, 772 cm⁻¹; ¹H-NMR (400 MHz, CDCl₃): δ 1.09 (t, *J* = 7.6Hz, 3H), 1.83-1.90 (q, 2H), 2.58 (s, 3H), 3.98 (t, *J* = 6.8Hz, 2H), 6.58 (s, 1H), 6.94-6.98 (m, 3H), 7.10-7.13 (m, 1H), 7.28-7.32 (m, 1H), 7.49 (d, *J* = 8.4 Hz, 1H), 8.33 (s, 1H); ¹³C-NMR (100 MHz, CDCl₃): δ ppm 9.01, 10.57, 22.50, 22.51, 70.09, 96.05, 113.61, 114.66, 120.01, 121.41, 122.46, 125.50, 125.68, 127.79, 129.10, 140.26, 142.97, 154.91, 160.24, 160.30; Anal. calc. for C₁₉H₁₈Cl₂N₂O₃; C,58.03; H,4.61; N,7.12; found: C,57.98; H,4.56; N,7.08; ESI-MS: 392.85 [M⁺].

2.6 Biological activity screening

2.6.1 MTT assay:

The half minimal inhibitory concentration was evaluated using MTT [3-(4,5-dimethylthiazol-2-yl)-2,5-diphenyltetrazolium bromide] assay as per standard protocol, used previously in Durgapal *et al.* [22] Cells were plated in a 96-well plate (1 x 10⁴ cells/well) and incubated overnight in DMEM media supplemented with 10% FBS. Each compound was added in 0.5, 1, 10, 25, 50, 75, 100 μM conc. and incubated further for 48hours. 20 μl of MTT solution (5 mg/mL in PBS) was added and plate was further incubated for 4 hours. Supernatant solution was removed and the blue formazan was dissolved in 100μl of acidified isopropanol. The absorbance was measured using microplate reader at 570 nm (Metertech Σ960)

Cell viability (%) = (average absorbance of treated groups/average absorbance of control group) × 100%. IC₅₀ values were calculated using Graph Pad Prism. Each experiment was performed in triplicates.

2.6.2 Trypan blue:

5×10^5 cells per well were seeded in 12 well plate and kept overnight for attachment. Next day, the respective cells were treated with IC₅₀ conc. of compounds (**12b** and **10d**), DMF and TritonX- 100 and were incubated for 48 hours. DMF treated cells were taken as vehicle control and TritonX- 100 as positive control. Following incubation, the supernatant was removed and adherent cells were collected. The cells were diluted with 0.4% trypan blue (1:1 ratio) and immediately counted on hemocytometer. Each experiment was performed in triplicates. Result expressed as percentage cell death [23].

2.6.3 LDH assay:

Lactate dehydrogenase enzyme remains in cytoplasm, however during necrosis due to plasma membrane damage it leaches out. Cells were plated on 96 well plate (1×10^4 cells/well) for 24 hours in DMEM media without phenol red, then compounds **12b** and **10d** were added in the 0.5, 1, 10, 25, 50, 75, 100 μ M concentration range. Subsequently, they were incubated for 48 hours. Assay was performed according to the manufacture's instruction (Pierce LDH Cytotoxicity Assay, Thermo Scientific, USA). Absorbance was measured at 490 nm in a microplate reader and percentage cytotoxicity was calculated.

2.6.4 Ethidium bromide/acridine orange staining assay:

Morphological changes due to apoptosis and necrosis were visualized using EtBr/AO staining technique. Respective cells were treated with IC₅₀ concentration of compound **12b** and **10d** for 48 hours. Triton- X 100 was used as positive control. Post-treatment, Cells were stained with EtBr and AO solution (100 μ g/ml in 1:1 ratio). Cells to stain ratio was maintained as 1:25 μ l. 10 μ l of cell suspension was placed on microscopic slide and images were taken using Leica DM 2500 fluorescence microscope fitted with Leica EZ camera.

2.6.5 DCFH-DA assay:

Dichlorodihydrofluorescein diacetate (DCFH-DA) staining was done to quantitate the intracellular ROS level in post treatment of derivative in both the cell line (A549 and MCF-7). For ROS estimation using Fluorimetry, 5×10^5 cells/well were seeded in 6 well plates overnight. The next day, the respective cells were treated with the IC₅₀ conc. of compound **12b** and **10d** and incubated for 48 hours. Following incubation, the experiment was performed as per the protocol described earlier in Umar *et al.*, [24].

2.6.6 In-silico based ADME and Toxicity study:

The drug-likeness prediction of compounds was done using Lipinski rule of five or criteria of four [25] retrieved from webserver tool SwissADME [26]. The structures of compound **12b** and **10d** were converted to canonical SMILES format and uploaded to SwissADME prediction

(<http://www.swissadme.ch>). The Toxicity prediction of compound was done using ProTox-II¹⁸ using chemical structure of the compound. The oral toxicity, the organ toxicity and toxicity end-point (hepatotoxicity, cytotoxicity, carcinogenicity, mutagenicity and immunotoxicity) were predicted using ProTox-II. The compounds are given different toxicity classes, depending on their LD₅₀ (mg/kg), which are defined according to the globally harmonized system of classification in labelling of chemicals (GHS).

2.6.7 Computational method:

On a computer with a Pentium IV CPU and Gaussian 09 software, all computations for the analyzed derivatives were completed. DFT/B3LYP methods were used in the computations with the 6-31 G (d, p) basis set. Without imposing any molecular symmetry restrictions, the geometries were optimized by minimizing the energies with respect to all geometrical parameters. The optimized geometries' structures have been depicted using GaussView. The same level of theory was also applied to frequency computations. In the geometry optimization processes, all structures were shown to be stationary points by the frequency calculations, and none of the vibrational analyses.

2.7 References

- [1] Z. Khan, P. S. Bisen, S. *Biochim. Biophys. Acta - Rev. Cancer*, **2013**, 1836, 123.
- [2] J. N. Soni, S. S. Soman, *Eur. J. Med. Chem.*, **2014**, 75, 77.
- [3] K. Kawasaki, ichi, M. Masubuchi, K. Morikami, S. Sogabe, T. Aoyama, H. Ebiike, H, S. Niizuma, M. Hayase, T. Fujii, K. Sakata, *Bioorg. Med. Chem. Lett.*, **2003**, 13, 87.
- [4] P. Yadav, P. Singh, A. K. Tewari, *Bioorg. Med. Chem. Lett.*, **2014**, 24, 2251.
- [5] K. Chand, Rajeshwari, A. Hiremathad, M. Singh, M. A. Santos, R.S. Keri, *Pharmacol. Reports*, **2017**, 69, 281.
- [6] H. Khanam, Shamsuzzaman. *Eur. J. Med. Chem.*, **2015**, 97, 483.
- [7] X. Y. Li, B. F.He, H. J. Luo, N. Y. Huang, W. Q. Deng, *Bioorg. Med. Chem. Lett.*, **2013**, 23, 4617.
- [8] M. Choi, H. Jo, H. J. Park, A. Sateesh Kumar, J. Lee, J. Yun, Y. Kim, S. B. Han, J. K. Jung, J. Cho, H. Lee, *Bioorg. Med. Chem. Lett.*, **2015**, 25, 2545.
- [9] M. Hranjec, I. Sović, I. Ratkaj, G. Pavlović, N. Ilić, L. Valjalo, K. Pavelić, S. Kraljević Pavelić, G. Karminski-Zamola, *Eur. J. Med. Chem.*, **2013**, 59, 111.
- [10] Xu, X. li; Yang, Y. rui; Mo, X. fei; Wei, J. lian; Zhang, X. jin; You, Q. dong. *Eur. J. Med. Chem.*, **2017**, 137, 45.
- [11] M. M.; Al-Sanea, G. H Al-Ansary, Z. M Elsayed, R. M. Maklad, E. B.; Elkaeed, M. A Abdelgawad, N. A. Bukhari, M. M. Abdel-Aziz, H. Suliman, W. M. Eldehna,. *J. Enzyme Inhib. Med. Chem.*, **2021**, 36, 987.
- [12] S. Karandikar, R. Soni, S.S.Soman, S.Umar, B.Suresh, *Synth. Commun.*, **2018**, 48, 2877.
- [13] S. D. Durgapal, S. S. Soman, *Synth. Commun.*, **2019**, 49, 2869.
- [14] D. Trachootham, Y. Zhou, H. Zhang, Y. Demizu, Z. Chen, H. Pelicano, P. J. Chiao, G. Achanta, R. B. Arlinghaus, J. Liu, *Cancer Cell*, **2006**, 10, 241.
- [15] R. Reinehr, S.Becker, A. Eberle, S. Grether-Beck, D. Häussinger, *J. Biol. Chem.*, **2005**, 280, 27179.
- [16] M. R. Ramsey, N. E. Sharpless, *Nat. Cell Biol.*, **2006**, 8, 1213.
- [17] S. Sakkiah, K. W. Lee, *Acta Pharmacol. Sin.*, **2012**, 33, 964.
- [18] M. N. Drwal, P. Banerjee, M. Dunkel, M. R. Wettig, R. Preissner, *ProTox: Nucleic Acids Res.*, **2014**, 42, 3.

- [19] I. Hayakawa, R. Shioya, T. Agatsuma, H. Furukawa, S. Naruto, Y. Sugano, *Bioorg. Med. Chem. Lett.*, **2004**, *14*, 455.
- [20] J. He, X. M.Tang, T.T. Liu, F. Peng, Q. Zhou, L. W. Liu, M. He, W.Xue, *Chem.Pap.*, **2021**, *75*, 1021.
- [21] Z. W. Mao, X. Z.heng, Y. P. Lin, C. Y. Hu, X. L Wang, C. P Wan, G. X. Rao, *Bioorg. Med. Chem. Lett.*, **2016**, *26*, 3421.
- [22] S. D. Durgapal, R. Soni, S. Umar, B. Suresh, S. S. Soman, *ChemistrySelect*, **2017**, *2*, 147.
- [23] A. I. Elkady, *Genet. Mol. Biol.*, **2013**, *36*, 12.
- [24] S. Umar, R. Soni, S. D. Durgapal, S. Soman, S. Balakrishnan, *J. Biochem. Mol. Toxicol.*, **2020**, *34*, e22553.
- [25] C.A. Lipinski, *Drug Discov. Today Technol.*, **2004**, *1*, 337.
- [26] A. Daina, M. C. Blatter, V. Baillie Gerritsen, P. M. Palagi, D. Marek, I. Xenarios, T. Schwede, O. Michielin, V.Zoete, *J. Chem. Educ.*, **2017**, *94*, 335.